



Teze disertace
k získání vědeckého titulu „doktor věd“
ve skupině věd: *fyzikálně-matematických*

Thesis aiming at the Research Professor (DSc.) degree

Soft-mode spectroscopy of ferroelectrics and multiferroics

Komise pro obhajoby doktorských disertací v oboru
Fyzika kondenzovaných systémů

Jméno uchazeče: **RNDr. Stanislav Kamba, CSc.**

Pracoviště uchazeče: Fyzikální ústav Akademie věd České republiky,
Na Slovance 2, 182 21 Praha 8

Místo a datum: Praha, březen 2021

Acknowledgment: The results presented in this dissertation are outcomes of research I have done or led in the Department of Dielectrics for the last 25 years. I would like to thank especially my former supervisor Jan Petzelt, but also all other members of our department who participated in the measurements and interpretation of results. I will list them in alphabetical order: Viktor Bovtun, Elena Buixaderas, Fedir Borodavka, Jan Drahokoupil, Veronica Goian, Ivan Gregora, Jiří Hlinka, Christelle Kadlec, Filip Kadlec, Martin Kempa, Petr Kužel, Dmitry Nuzhnyy, Maxim Savinov, Stella Skiadopoulou, Volodymyr Skoromets, Ivan Rychetský, Přemysl Vaněk, Jakub Vít and Vladimír Železný. I measured and independently evaluated IR spectra only till 2005. Since that time, when I became head of the research group, I mostly managed and led the research, collected all the results, interpreted them and wrote the papers.

I also benefited from a fruitful collaboration with the groups of Prof. D. Schlom (Cornell University, USA), Prof. Greenblatt (Rutgers University, USA), Prof. G. Schaack (University Würzburg, Germany), Prof. J. Banys (Vilnius University, Lithuania), Prof. B. Malič (Jožef Stefan Institute, Ljubljana, Slovenia), dr. Belik (NIMS Tsukuba, Japan), dr. K. Maca and dr. K. Kachlík (CEITEC BUT, Brno), who provided us high-quality samples.

Contents

Contents.....	3
1. Introduction	4
2. Scientific background.....	6
3. Investigation of tatrates – hydrogen bonded ferroelectrics	9
4. Lead-based relaxor ferroelectrics	12
6. Soft-mode spectroscopy in multiferroics with displacive ferroelectric phase transitions ...	20
7. Spin-induced multiferroics	27
8. Resume	30
9. References.....	31
10. List of papers.....	38

1. Introduction

Let us start first with a short historical remark. The concept of FE soft mode, i.e. one or several polar phonons, whose frequency tends to zero or greatly decrease near the temperature of structural PT T_c , is very old and it is frequently used for explanation of dynamics of the PTs. Classical Cochran's papers^{1,2,3} from 1959-1961 are usually considered as the first papers about this topic, but Anderson⁴ came with the idea of soft mode already in 1958. He published his paper only in Russian and although the paper appeared only in conference proceeding two years later,⁴ it is rather frequently cited in Eastern Europe. Nevertheless, one must accept, that the first original ideas about the FE soft mode were published by Ginzburg already in 1949,^{5,6,7} but at that period the Russian papers were not translated to English, therefore these articles were forgotten.

First observation of the soft mode is even older. Landsberg and Mandelstam⁸ saw some soft mode in Raman spectra near the $\alpha \leftrightarrow \beta$ transition in quartz already in 1929, but they explained its temperature behaviour inaccurately. Therefore the papers of Barker and Tinkham,⁹ as well as of Cowley¹⁰ published in 1962, are considered as the first papers, which experimentally confirmed the soft mode theory. Let us note that both papers concern the study of quantum paraelectric SrTiO₃ above 90 K. By the way, most of experimental works in 1960's refer to soft mode studies of quantum paraelectrics SrTiO₃ and KTaO₃ probably due to the relatively high soft mode frequency and large temperature changes observed in these materials. Regarding the experimental techniques, mostly inelastic neutron scattering and Raman scattering were used. Far infrared (IR) spectroscopy was less used, but it became to be more popular in the 1970's with the development of fast Fourier spectroscopy. Nevertheless, this technique is more appropriate than other techniques, because the soft mode is IR active in both paraelectric and FE phase, in contrast to Raman scattering, where the soft mode is mostly active only in the FE phase or it can be activated in paraelectric phase by an external electric field. Inelastic neutron scattering has the advantage that it allows to measure dispersion of the soft optical phonon branch in the whole Brillouin zone, but this measurement is much more time consuming, matchlessly more expensive and moreover large single crystals are needed for such experiments.

In the beginning of 1970's, the soft mode spectroscopy was used already frequently for the study of dynamics of phase transitions – see the review papers^{11,12} and a monography¹³. It was shown that the optical soft mode is a dynamical origin of only displacive structural PTs. In the case of order-disorder PTs (see below), the soft mode is not an optical phonon, but it has a

relaxational character and slowing down of the relaxation frequency is seen in microwave (MW), radio- or low-frequency ranges on cooling towards T_c .¹²

Our laboratory in the Institute of Physics, Czech Academy of Sciences, has a long tradition in investigation of the FE soft modes thanks to J. Petzelt, who was active in this field since 1966. In 1983 the laboratory was equipped with a new Fourier Transform spectrometer Bruker IFS 113v (equipped with He-cooled bolometer) and in the same time I started my diploma work with this instrument. The work dealt with a far IR investigation of phonons near the incommensurate PT in BaMnF₄.¹⁴ Later on, I wrote my PhD thesis in the same lab. The work was devoted to the investigation of lattice dynamics in highly anharmonic KSCN crystal with an order-disorder PT,¹⁵ to betaine calcium chloride dehydrate^{16,17} (organic material with a sequence of 16 PT's to various commensurately and incommensurately modulated phases) as well as to high-temperature superconductors.^{18,19} In the beginning of 1990's, I was lucky to spend a longer stay at the ETH Zurich and at the University of Würzburg continuing in the field of IR studies of various ferroelectrics, in the latter case even with the help of high hydrostatic pressure. After my return back in 1995, our Prague lab was gradually developed with a new equipment (Raman and micro-Raman spectrometers, two impedance analysers covering the frequency range of 0.1 Hz – 1.8 GHz, network analyzer (50 MHz – 50 GHz) and mainly P. Kužel developed a time-domain THz spectrometer (100 GHz – 2.5 THz) based on a laser with ultrashort femtosecond pulses. All these instruments allowed us to cover practically continuously the spectral range from 0.1 Hz up to 150 THz. Moreover, most of the measurements are possible to be carried out in a broad temperature range 5 - 900 K. Such a unique equipment ranks our lab in the front of world laboratories working in the field of dielectric spectroscopy.

Demand of miniaturization of the new capacitors in integrated circuits requires new dielectric materials with high permittivity. In the case of non-volatile memories the capacitors or transistor gates should be moreover FE. However, the permittivity in ceramics and thin films is markedly reduced compared to the single crystals due to the low-permittivity grain boundaries, dead layers between the thin films and substrates, as well as due to the strain in the films caused by a misfit between the substrates and films.²⁰ Understanding the permittivity reduction is necessary for processing good quality thin films and ceramics and broad-band dielectric spectroscopy helps a lot in this case.

In the 1990's a giant piezoelectric effect was revealed in FE relaxor-based single crystals, which allowed construction of new and much more efficient piezoelectric devices. Since that time the interest in relaxors rapidly increased and mainly the broad-band dielectric spectroscopy

(including of our works) contributed a lot in understanding of the mechanisms of giant piezoelectric effect and structural PTs in these materials.

Within the last 25 years we investigated dynamics of structural PTs in many FE materials, which allowed us to generalize the soft mode behaviour: In reality the SM never softens completely, some finite frequency can be observed at T_c . Several reasons can be given for the softening saturation:²¹

- First-order nature of the structural PT.
- Quantum effects at low temperatures in incipient ferroelectrics.
- Polar soft mode is not the critical soft mode of the PT. The proper soft mode is coming from outside of the Brillouin zone centre. This is the case of antiferroelectric PT's, incommensurate FE transitions or improper FE PTs.
- The most frequent case is that the central mode type dispersion (in other words, a dielectric relaxation) appears near T_c below the optical SM frequency. Both modes are coupled and the central mode is mainly responsible for the dielectric anomaly near T_c . This case occurs due to defects or more often at the crossover from the displacive to order-disorder type PTs.

In this work we will review results mostly from the last 25 years.

2. Scientific background

In usual proper ferroelectrics, the low-frequency permittivity above the second order PT temperature T_c follows the Curie-Weiss law¹³

$$\varepsilon' = \frac{C}{(T-T_c)} \quad (1)$$

where C is the Curie-Weiss constant. The complex permittivity $\varepsilon^* = \varepsilon' + i\varepsilon''$ is determined by a sum of contributions of the high-frequency electronic polarization (ε_∞), polar phonons (ε_{ph}) and possibly of some dielectric relaxations (ε_{dr}), which can be usually expressed as a sum of damped harmonic oscillators and Debye relaxations:¹³

$$\varepsilon^*(\omega) = \varepsilon_\infty + \varepsilon_{ph} + \varepsilon_{dr} = \varepsilon_\infty + \sum_j^n \frac{\Delta\varepsilon_j \omega_{TOj}^2}{\omega_{TOj}^2 - \omega^2 + i\omega\gamma_j} + \sum_j^m \frac{\Delta\varepsilon_{Rj} \omega_{Rj}}{\omega_{Rj} + i\omega} . \quad (2)$$

ω_{TOj} , γ_j and $\Delta\varepsilon_j$ denote the transverse frequency, damping and dielectric contribution to the static permittivity of the j -th polar phonon, respectively, and $\Delta\varepsilon_{Rj}$ and ω_{Rj} mark the dielectric strength and relaxation frequency of the j -th relaxation, respectively. In the case of displacive PTs, the relaxation contribution ε_{dr} should be zero in the paraelectric phase and the increase in

permittivity near T_c (see Eq. 1) is caused by softening (i.e. decrease of the frequency) of one of the polar phonons. If the phonons are not coupled, the oscillator strengths $f_j = \Delta\varepsilon_j \omega_{\text{TO}j}^2$ of all polar modes are expected to be roughly temperature independent. It means, for example, that if the soft mode frequency ω_{SM} reduces twice, $\Delta\varepsilon_{\text{SM}}$ increases four times, etc. Temperature dependence of the ω_{SM} can be easily obtained from the Curie-Weiss law (Eq. 1) and Lyddane-Sachs-Teller relation,²² which expresses the relation between static permittivity ε_0 and high frequency permittivity ε_∞ with longitudinal ω_{LO} and transverse ω_{TO} phonon frequencies. For materials with two atoms per unit cell, it has the form²²

$$\frac{\varepsilon_0}{\varepsilon_\infty} = \frac{\omega_{\text{LO}}^2}{\omega_{\text{TO}}^2}. \quad (3)$$

ε_∞ and ω_{LO} are usually only slightly temperature dependent and because ε_0 diverges at T_c (see Eq. 1), transverse phonon frequency ω_{TO} should decrease to zero at T_c . If we assume ε_∞ and ω_{LO} constant and if we put $\omega_{\text{TO}} = \omega_{\text{SM}}$, we obtain Cochran law for the temperature dependence of the soft mode frequency¹

$$\omega_{\text{SM}}^2 = A(T - T_c) \quad (4)$$

where A is the Cochran constant. For materials with more atoms per unit cell, the generalized Lyddane-Sachs-Teller relation has the form¹³

$$\frac{\varepsilon_0}{\varepsilon_\infty} = \prod_{j=1}^n \frac{\omega_{\text{LO}j}^2}{\omega_{\text{TO}j}^2}. \quad (5)$$

In the case of non-coupled phonons only one transverse phonon frequency is temperature dependent and one can obtain again the Cochran law (Eq. 4). Although the concept of the optical soft mode as the dynamical origin of the PT is accepted since 1960, there are only several pure displacive ferroelectrics known (e.g. PbTiO_3 ²³), where the low-frequency dielectric anomaly is caused only by softening of the optical soft mode. Also for pure incipient ferroelectrics like SrTiO_3 ,^{9,24,25} and KTaO_3 ,^{24,26} where the soft mode does not soften completely, because the FE PT is not reached in these materials, the soft mode is completely responsible for the anomalous temperature dependence of the low-frequency permittivity.

If the high-temperature paraelectric structure is disordered, i.e. if some kind of atoms occupy two or more equivalent positions with the probability less than 1, the atoms usually order below T_c only in some of the mentioned sites and we say that the system undergoes an order-disorder phase transition at T_c . If the ordering of ions is connected with appearance of spontaneous polarization, the PT is FE. In this case the phonons may exhibit only small temperature

anomalies and the dynamical origin of the PT is the critical slowing-down of some relaxation frequency ω_{Rj} (see the last term in Eq. 2) near T_c , which expresses the hopping motion of the disordered atoms among the equivalent positions in paraelectric phase. The soft relaxation frequency ω_{Rs} in the disordered materials plays the role of the optical soft mode in displacive ferroelectrics and follows the simple linear temperature dependence above T_c ¹²

$$\omega_{Rs} = A'(T - T_c). \quad (6)$$

Below T_c the soft dielectric relaxation usually disappears from the spectra, but another relaxation may appear due to dynamics of FE domain walls. If we take into account that the relaxation frequency cannot increase up to infinity on heating, we should add to the linear dependence (Eq. 6) some saturation frequency ω_{sat} . Modified law for the soft relaxation frequency has than the form²⁷

$$\omega_{Rs}^{-1} = [A'(T - T_c)]^{-1} + \omega_{sat}^{-1} \quad (7)$$

Relaxation strength $f_{Rs} = \Delta\epsilon_{Rs}\omega_{Rs}$ of the soft relaxation in the paraelectric phase can be assumed temperature independent and due to the slowing down of ω_{Rs} one can obtain the Curie-Weiss increase of the static permittivity. Typical examples of materials with order-disorder PT are KDP-type ferroelectrics, triglycine sulphate or sodium nitrite.^{12,13}

Many materials were reported as classical displacive or order-disorder ferroelectrics, however their detailed investigations have shown that they usually exhibit some crossover between both kinds of mechanism of the PTs. For example, an underdamped optical soft mode was observed in the THz spectra of tris-sarcosine calcium chloride (TSCC),²⁸ therefore this material was assumed to be displacive FE. However, the careful reinvestigation of the THz spectra of TSCC and comparison with the low-frequency dielectric data revealed a soft relaxation (central mode) close to T_c which is responsible for critical deviations from the Curie-Weiss law and the Cochran law near T_c .²⁹ The central mode was assigned to critical polar cluster dynamics. On the other hand, also many ferroelectrics with order-disorder PTs show critical slowing down of the relaxation which is coupled with optical phonons or other higher-frequency relaxations. It means that the driving force of the PT is the latter excitation, although the dielectric anomaly near T_c is mainly due to the soft relaxation. As the examples Rochelle salt³⁰ or $\text{LiNaGe}_4\text{O}_9$ ²⁷ can be named, which will be here discussed, other examples can be found in the reviews.^{12,20,31}

It seems nowadays that the PTs with a pure soft optical mode or a pure soft relaxation mode are rather rare. Most of materials exhibit crossover between displacive and order-disorder PT, i.e. the phonons exhibit anomalies near T_c , however their contributions to permittivity do not

explain the complete dielectric anomaly near T_c . Additional soft relaxation (i.e. central mode) frequently appears near T_c and only the sum of both contributions is responsible for the dielectric anomaly near T_c .

3. Investigation of tatrates – hydrogen bonded ferroelectrics

Sodium potassium tartrate tetrahydrate $\text{NaKC}_4\text{H}_4\text{O}_6 \cdot 4\text{H}_2\text{O}$, called Rochelle salt (RS), is the first known ferroelectrics. Joseph Valashek revealed a FE hysteresis loop in this compound already in 1920,³² but published in detail in 1921.³³ Although RS was studied by many authors within the last 100 years, the understanding of the mechanism leading to the formation of a state with a spontaneous polarization was a long time puzzling. In contrast to all other ferroelectrics, its FE phase (monoclinic space group $\text{P}2_1-\text{C}_2^2$, $Z=4$) exists only between $T_{C1}=255$ K and $T_{C2}=297$ K. Above and below these temperatures, RS is paraelectric with the same orthorhombic space group $\text{P}2_12_12-\text{D}_2^3$, $Z=4$. Older neutron diffraction data³⁴ showed that the whole tartrate and crystal water molecules are disordered in the paraelectric phase with a small disordering amplitude. Newer reinvestigation using synchrotron x-ray diffraction revealed a disorder of only K atoms and three water O atoms in the paraelectric phase, while the bonded H atoms in water are not disordered.³⁵ A Debye relaxation mode was observed in the MW region and its relaxation frequency linearly decreases with temperature near T_{C1} and T_{C2} ,^{36,37,38} therefore the PTs in RS were regarded as classical examples of the order-disorder type.

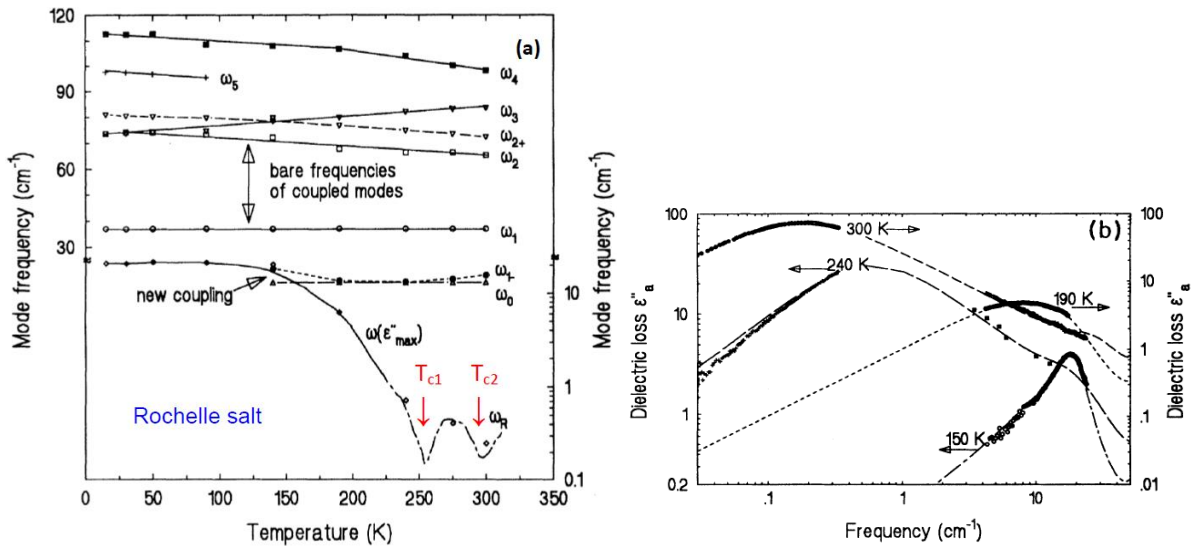


Fig. 1. Left: Temperature dependence of the mode frequencies obtained from the fit of $E||a$ polarized spectra with the coupled-oscillator model. Modes with the bare frequencies ω_1 and ω_2 are coupled below 140 K, while the modes with frequencies ω_1 and ω_0 are coupled at higher temperatures and this coupling induces a soft critical dielectric relaxation ω_R near both T_{C1} and T_{C2} . b) Dielectric loss spectra ϵ''_a obtained from the fits of experimental microwave³⁹ and THz⁴⁰ spectra. From Ref. 30.

However, later it was shown that at low temperatures the relaxation hardens to the THz range and remarkably underdamps, so that it has phonon (i.e. resonant) character.⁴⁰ Because its oscillator strength $f_{SM} = \Delta\epsilon_{SM}\omega_{SM}^2$ is reduced on cooling below T_{C1} by one order of magnitude, Volkov et al.⁴¹ suggested that this mode is probably linearly coupled with another optical phonon in the FIR range. It means that the transition is more likely displacive than order-disorder.

We have investigated the lattice dynamics of RS by means of IR, Raman and inelastic neutron scattering spectroscopies.^{30,42} We have really observed the soft mode near 20 cm^{-1} which is linearly coupled with the mode near 75 cm^{-1} (see Fig. 1). The higher frequency mode partially softens on heating from low temperatures to T_{C1} and it causes the softening and rising damping of the mode near 20 cm^{-1} . Moreover, the soft mode near 20 cm^{-1} is coupled to an overdamped mode with temperature independent bare frequency 13 cm^{-1} . Temperature dependent coupling of these modes causes critical slowing down of the dielectric relaxation, which is responsible for the strong dielectric anomalies seen near T_{C1} and T_{C2} . It means that the dynamical origin of the FE PTs in RS is not only a dielectric relaxation, but also unstable optical phonons near 20 and 75 cm^{-1} . Therefore the PTs in RS can be treated as a mixture of displacive and order-disorder type.³⁰ This conclusion was also confirmed by IR measurements at high hydrostatic pressures, where we observed the largest influence of the pressure on the phonon of frequency near 75 cm^{-1} ,⁴³ i. e. the mode which induces softening of the modes in THz and MW regions depicted in Fig. 1.

Chemically relative to RS is lithium thallium tartrate monohydrate (LTT) – $\text{LiTlC}_4\text{H}_4\text{O}_6\cdot\text{H}_2\text{O}$. It exhibits only one FE PT and its critical temperature $T_c=11\text{ K}$ is one of the lowest known.⁴⁴ The free permittivity ϵ'_a obeys the Curie-Weiss law well above T_c , but in contrast to other ferroelectrics, ϵ'_a decreases only slightly below T_c .⁴⁵ The permittivity is very sensitive to the mechanical boundary condition, so whereas ϵ'_a reaches ~ 5000 at T_c , the clamped $\epsilon'_a(T_c)$ is only ~ 30 .⁴⁶ Both the elastic compliance at constant electric field s_{44}^E and the piezoelectric coefficient d_{14} become exceedingly large close to T_c (note that LTT is piezoelectric already in the paraelectric phase above T_c) and appear to have the highest magnitude measured in any materials.⁴⁶

The optical soft mode in LTT was first observed in far IR spectra by Gerbaux *et al.*⁴⁷ and investigated in more details by Volkov *et al.*⁴⁸ The latter authors have shown that its frequency

softens from 21 cm^{-1} at 300 K to 9 cm^{-1} at T_C , but its dielectric contribution $\Delta\epsilon$ was two orders of magnitude smaller than the observed free permittivity near T_C . Therefore Volkov *et al.*⁴⁸ claimed that another dispersion of the relaxation type should exist in the MW region and the PT is of mixed displacive and order-disorder type. Nevertheless, Hayashi *et al.*⁴⁹ have shown that the free ϵ'_a is enhanced due to piezoelectric resonances in the MW region and that the high frequency permittivity corresponds very well to the THz $\epsilon'_a(T)$.⁴⁸ Therefore the PT is purely displacive, although the optical soft mode does not soften completely due to its strong coupling with a transverse acoustic mode.

Piezoelectric paraelectric phase has an orthorhombic structure ($P2_12_12 - D_2^3, Z=4$),^{50,51} but the structure of FE phase was not known. Therefore we performed a new IR, Raman, dielectric and structural measurements of LTT. From the high-pressure dielectric data we have shown that T_C strongly increases with hydrostatic pressure (up to 54 K at 370 MPa).⁵² Permittivity $\epsilon'_a(T)$ exhibits an unusual plateau below T_C and then drops down in dependence on pressure by 5-15 K below T_C (Fig. 2). FE hysteresis loops are only slim in the range of plateau, giving evidence about easy movement of domain walls, but below the temperature of the drop down (T_{C2}) the domains are frozen and the sample cannot be switched. The unusual temperature independence of ϵ'_a seen between T_C and T_{C2} was theoretically explained by Tagantsev with a bilinear coupling between the order parameter (soft mode) and strain.⁵³ The optical soft mode is strongly temperature and pressure dependent. It exhibits minimum frequency at T_c but no anomaly near T_{C2} ,⁵² i.e. no structural change occurs at T_{C2} , only the coupling between the soft mode and strains changes. We performed also an elastic neutron scattering experiment at hydrostatic pressure

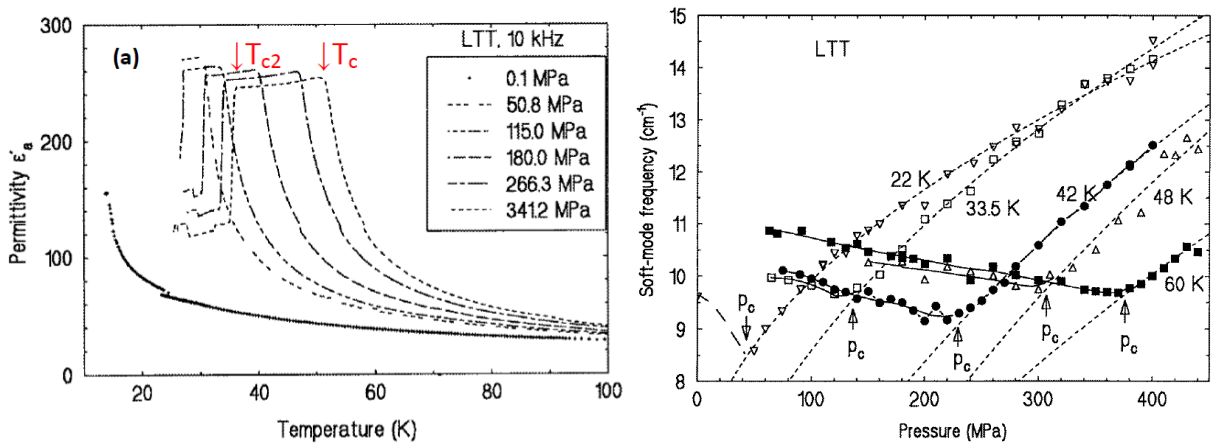


Fig. 2. Left: Temperature dependence of the permittivity ϵ'_a of LTT at various pressures. Right: Pressure dependence of the soft-mode frequencies at different temperatures obtained from the Raman b(cb)c spectra. The broken curves in the high-pressure FE phase are results of the square-root fits (equivalent to the Cochran law as a function of pressure). From Ref. 52.

of 120 MPa with the purpose to determine symmetry of the FE phase.⁵⁴ We obtained monoclinic FE structure with a symmetry $P2_111$ below both T_C and T_{C2} , with a larger monoclinic distortion below T_{C2} than below T_C .

Chemically related to LTT is lithium ammonium tartrate monohydrate (LAT). It exhibits the FE and ferroelastic PTs at $T_c=98$ K. We investigated IR and Raman spectra of the LAT down to 15 K and no soft mode was observed,⁵⁵ because the PT is proper ferroelastic and improper FE. In contrast to LTT where a substantial increase of T_c with hydrostatic pressure was observed, in case of the LAT crystal T_c decreases only slightly down to 91 K at 400 MPa.⁵⁵

4. Lead-based relaxor ferroelectrics

Unlike classic ferroelectrics which exhibit a peak in permittivity $\epsilon'(T)$ at the temperature of PT, which is frequency independent in displacive ferroelectrics or its height depends on frequency, but its temperature T_C does not change (in case of order-disorder PTs), there is another class of materials, which exhibits a high and frequency dependent peak in $\epsilon'(T)$ – see e.g. Fig. 3. These materials frequently do not exhibit any FE PT without external electric field, but since they show many similarities with ferroelectrics, they are called relaxor ferroelectrics.

Since the discovery of the first relaxor FE $\text{PbMg}_{1/3}\text{Nb}_{2/3}\text{O}_3$ (PMN) by Smolenskii and Agranovskaya⁵⁶ in the end of 1950th, many materials with similar dielectric properties were found. Isupov⁵⁷ tried to explain the peculiar dielectric anomaly in relaxors by a diffuse PT, i.e. by a distribution of the FE PT temperatures due to microscopic inhomogeneities in the samples. Nevertheless, later it was shown that the relaxor dielectric anomaly is not necessary caused by

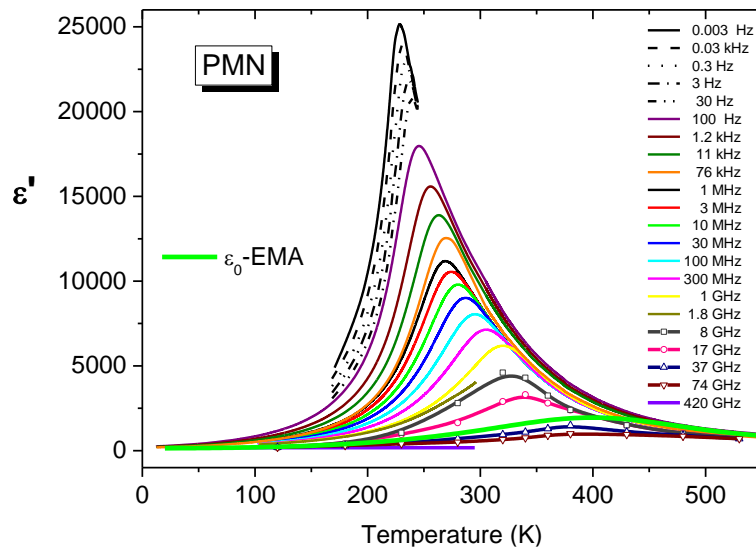


Fig. 3. Temperature dependence of permittivity in relaxor FE $\text{PbMg}_{1/3}\text{Nb}_{2/3}\text{O}_3$ depicted at various frequencies. ϵ_0 -EMA curve is result of calculation of the phonon static ϵ_0 using effective medium approximation described in Ref. 82. Modified after Ref. 79.

a PT. For example, model relaxor FE PMN exhibits non-polar cubic structure down to liquid helium temperatures⁵⁸ and it becomes FE only under cooling in bias electric field.⁵⁹ In 1983 Burns and Dacol measured temperature dependences of the optical refractive index in various relaxors and observed a deviation from the linear temperature dependence some 300 K above the temperature T_m , where $\epsilon'(T)$ shows maximum.⁶⁰ They explained it by a creation of polar clusters and since that time the temperature T_d is called the Burns temperature. Nowadays it is believed that most of peculiar physical properties of relaxors are somehow connected with the polar nanoclusters, which appear probably due to some quenched random electric fields⁶¹ from cations of different valences, which are sitting in the equivalent perovskite sites (e.g. Mg^{2+} and Nb^{5+} in PMN), however details are still not fully understood.

In 1997 Park and Shrout⁶² showed that relaxor-based $PbMg_{1/3}Nb_{2/3}O_3$ - $PbTiO_3$ (PMN-PT) and $PbZn_{1/3}Nb_{2/3}O_3$ - $PbTiO_3$ (PZN-PT) single crystals exhibit ultrahigh strain and piezoelectric behaviour in electric field, and since that time the interest for relaxors rapidly increased, because these materials show many technical applications in piezoelectric devices and microelectronics. Besides many research papers published on relaxors, also several reviews appeared. We can refer the reader to reviews of Cross,^{63,64} Ye,⁶⁵ Samara,^{66,67} Bokov,^{68,69} where the present knowledge of relaxors is overviewed. There are also several reviews about the lattice dynamics of relaxors. Results of Raman scattering were reviewed by Siny et al.⁷⁰, inelastic neutron scattering results by Shirane and Gehring⁷¹ and Cowley et al.⁷² IR and MW dielectric dispersion by Kamba and Petzelt,⁷³ Hlinka et al.⁷⁴ and Buixaderas et al.³¹

We have demonstrated that for understanding of peculiar dielectric dispersion in relaxors a broad-band dielectric spectroscopy from sub-Hz up to THz and IR frequencies is necessary. First of all, we investigated ceramics of lanthanum modified lead zirconate titanate $(Pb_{1-x}La_x)(Zr_yTi_{1-y})_{1-x/4}O_3$ (PLZT 100(x/y/1-y)) with $x = 8$ and 9.5 and $y = 65$.⁷⁵ Both ceramics exhibit a broad and strongly frequency dependent peaks in $\epsilon'(T)$ and $\epsilon''(T)$ seen between 325 K (at 100 Hz) and 500 K (at 36 GHz). A single broad and symmetric dispersion that occurs below the polar phonon frequencies, was fitted with the Cole-Cole formula and with the uniform distribution of Debye relaxations. On decreasing temperature, the distribution of relaxation times becomes extremely broad (10 orders of magnitude at 300 K in PLZT 9.5/65/35 - see Fig. 4 left) which indicates increasing correlation among the clusters. The mean (τ_0) and upper (τ_1) relaxation times diverge according to the Vogel-Fulcher law⁷⁵

$$\tau_{0,1}(T) = \tau_L \exp\left(\frac{U_{VF}}{T-T_{VF}}\right) \quad (8)$$

with the same freezing temperature $T_{VF} = 230 \pm 5$ K for both ceramics, but different activation energies U_{VF} 1370 K and 1040 K for the PLZT 8/65/35 and 9.5/65/35, respectively. τ_L in Eq. (1) marks the limiting high-temperature relaxation time, which is of the order of the reciprocal lowest optical phonon frequency. The shortest relaxation time τ_2 is about 10^{-12} s and remains almost temperature independent (Fig. 4 left). Below room temperature, the loss spectra $\varepsilon''(\omega)$ become essentially frequency independent and the permittivity increases linearly with decreasing logarithm of frequency (Fig. 4 right).⁷⁶ This behaviour was successfully explained by a constant distribution $g(\tau)$ of equally strong Debye relaxations between upper (τ_1) and lower (τ_2) limits of relaxation times. We have shown that if the measured frequency range is much narrower than the distribution $g(\tau)$, the complex permittivity can be expressed as:⁷⁵

$$\varepsilon'(\omega) = \varepsilon_\infty - B(T) \ln(\omega\tau_2) \quad (9)$$

$$\varepsilon''(\omega) = \frac{\pi}{2} B(T)$$

where $B(T)$ is the frequency-independent but temperature-dependent parameter describing the magnitude of $g(\tau)$. This model was successfully used not only for description of the low-temperature dielectric properties of relaxor PLZT⁷⁵ (Fig. 4 right), PMN⁷⁹ and $\text{PbMg}_{1/3}\text{Ta}_{2/3}\text{O}_3$

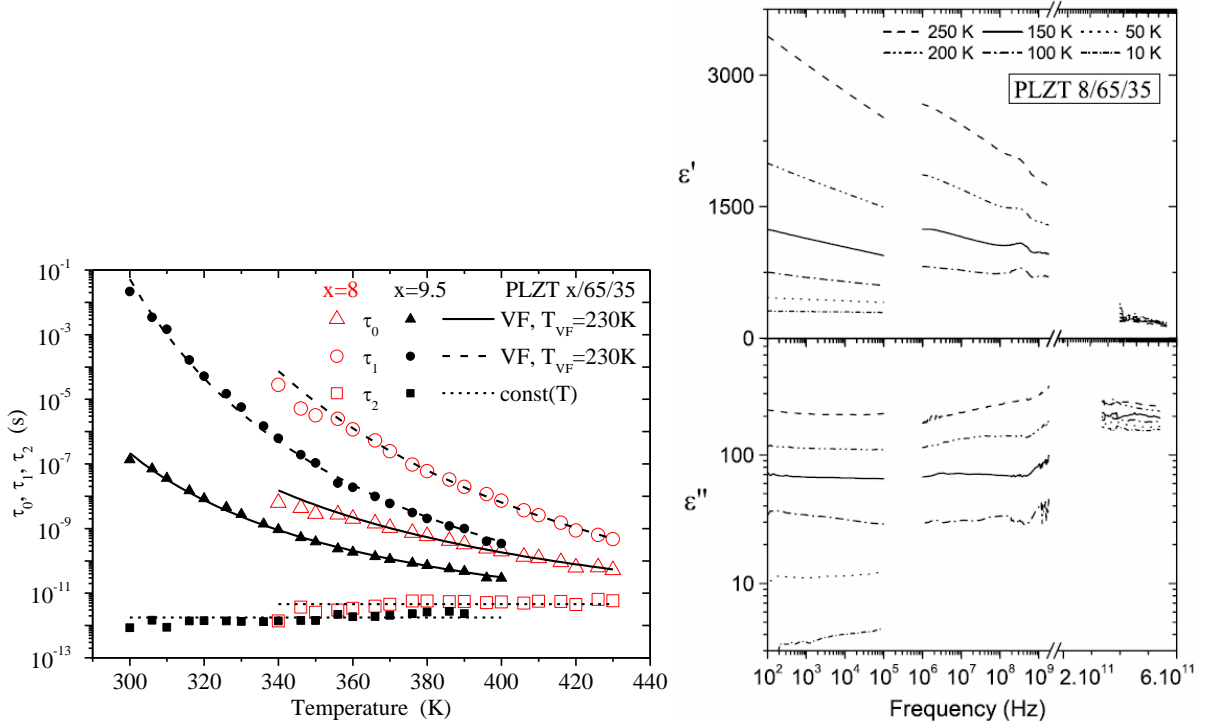


Fig 4. Left: Temperature dependence of the mean (τ_0), upper (τ_1) and lower (τ_2) relaxation times in relaxor PLZT determined from the uniform distribution model of Debye relaxation frequencies. Right: Frequency dependence of the real and imaginary parts of the complex permittivity in PLZT 8/65-35 at various temperatures close and below freezing temperature T_{VF} . After Refs. 75 and 76.

(PMT),⁷⁷ but also for fitting of the anomalous broad dielectric relaxation in $\text{Bi}_{1.5}\text{Zn}_{1.0}\text{Nb}_{1.5}\text{O}_7$ with cubic pyrochlore structure,⁷⁸ which is not a relaxor FE. In this case the upper relaxation time follows the Arrhenius law and the relaxation was assigned to the local hopping of atoms in the A and O' positions of the pyrochlore structure among several local potential minima.

The archetypical and best-studied relaxor FE is PMN because its solid solution with PbTiO_3 is material with the highest piezoelectric coefficients. Typical relaxor peak in $\epsilon'(T)$ measured between 3 mHz and 420 GHz is shown in Fig. 3.⁷⁹ Frequency plots of the dielectric function (Fig. 5) reveal similar behavior as in PLZT: a slowing down and broadening of the dielectric relaxation on cooling.⁸⁰ Again, in the logarithmic scale linearly dependent $\epsilon'(\omega)$ and frequency independent loss spectra $\epsilon''(\omega)$ are seen below the freezing temperature $T_{\text{VF}} \cong 230$ K. Qualitatively similar dielectric behavior was observed in all relaxors and we interpreted it as follows:⁸¹ The dielectric relaxation appears in the spectra below the Burns temperature ($T_{\text{d}} = 600 - 700$ K in various relaxors) and expresses a dynamical flipping of the cluster polarization. Below the freezing temperature T_{VF} the clusters freeze out and the flipping of polarization disappears. Nevertheless, the polar cluster boundaries can still vibrate (breeze) below T_{VF} , but since it is a temperature activated process over energy barriers with some distribution, the relaxation times (or frequencies) exhibit also a distribution $g(\tau)$, which broadens on cooling. This low-temperature $g(\tau)$ is responsible for the dielectric dispersion observed below T_{VF} (e.g. below 200 K in Fig. 5). Our recent detailed analysis of the dielectric dispersion between T_{VF} and T_{d} revealed two relaxations, which were well fitted using two Cole-Cole formulas which express the flipping and breezing of polar nanoregions.⁸² The former one disappears below T_{VF} (τ_1 diverges) and the latter one appears below T^* , where the static polar nanoclusters start to appear (depending of the material, $T^* = 350 - 450$ K) and its $g(\tau)$ anomalously broadens below the freezing temperature, as explained above.

Phonons in relaxor ferroelectrics were also frequently investigated. Inelastic neutron scattering spectra revealed a drop down of the soft optical phonon branch and its merging with an acoustic phonon branch at the critical wavevector q_{wf} and its disappearance below q_{wf} at temperatures between T_{VF} and T_{d} .⁸³ This effect was called a phonon waterfall and it was at first explained by a phonon scattering on the polar nanocluster boundaries.^{84,85} Our later inelastic neutron scattering studies found that the critical wave vector q_{wf} , below which the phonon waterfall appears, depends on the choice of the Brillouin zone and therefore the relation of q_{wf} to the size of the polar nanoregions is highly improbable.⁸⁶ We explained the phonon waterfall phenomena by a coupling of the acoustic and optical phonon branches. Observation of

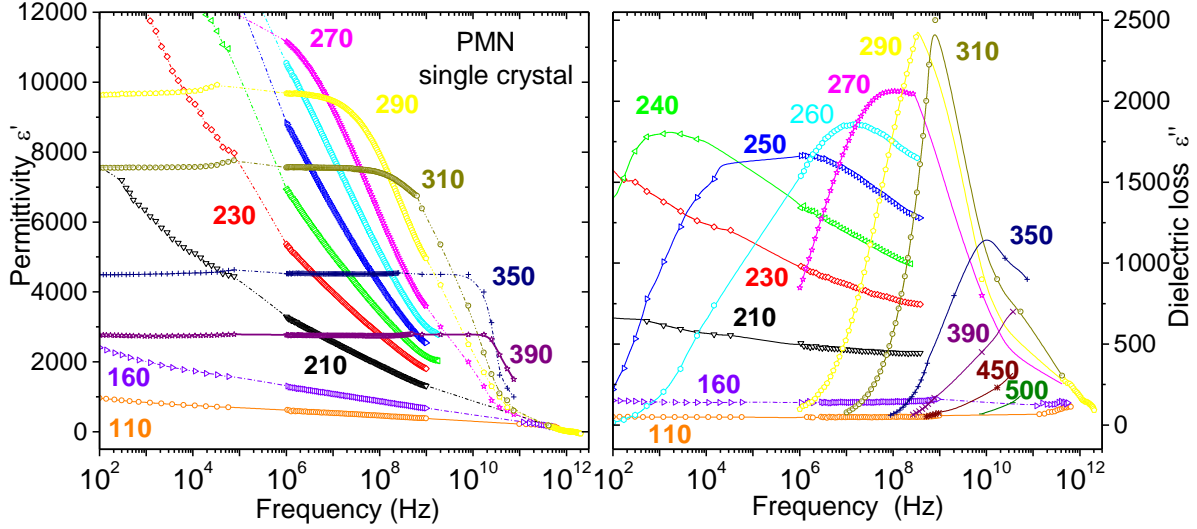


Fig. 5. Frequency dependence of real and imaginary parts of dielectric function in $\text{PbMg}_{1/3}\text{Nb}_{2/3}\text{O}_3$ taken at various temperatures. Modified from ref. 80.

different q_{wf} in various Brillouin zones was explained by different structure factors.⁸⁶

Nevertheless, below T_{VF} and above T_{d} , a soft optical phonon was observed in inelastic neutron scattering spectra of PMN with critical temperature around $T^* = 400$ K.⁸³ The same optical soft mode was also observed in the IR spectra, but in contrast to the inelastic neutron scattering spectra, the underdamped soft phonon was observed at *all* temperatures (including temperatures between T_{VF} and T_{d}) not only in PMN (Fig. 6),⁸⁷ but also in PLZT,⁷⁵ PMT⁷⁷ and $\text{PbSc}_{1/2}\text{Ta}_{1/2}\text{O}_3$.⁸⁸ Earlier spectroscopic data⁸⁷ have shown that below 400 K, the soft phonon in PMN follows the Cochran law with the extrapolated critical temperature corresponding to the Burns temperature T_{d} (Fig. 6a). Nevertheless, at higher temperatures the soft mode hardens slower than the Curie-Weiss law and the Lyddanne-Sachs-Teller relation describing the experimental $\varepsilon'(T)$ require. Moreover, an additional overdamped central mode was observed below T_{d} (Fig. 6a), whose activation was explained by a splitting of the soft mode due to a local breaking of cubic symmetry in polar clusters.⁸⁷ Based on inelastic neutron scattering experiments, Vakhrushev and Shappiro proposed the soft mode splitting also above T_{d} and they claimed that both components exhibit minimum near T_{d} , but their phonon parameters had high error bars due to the high phonon damping above T_{d} .

For that reason we have performed detail THz and IR studies of relaxor PMN and PMT up to 900 K and fitted the spectra to the Bruggeman effective medium formula.^{82,89} Six polar phonons observed at 900 K gave evidence about the non-cubic local structure above T_{d} , since the cubic perovskite structure allows only three polar phonons in the IR spectra. We clearly observed the *E*-component of the soft mode polarized perpendicularly to local polarization

($\mathbf{P}||[111]_{\text{cub}}$) in polar nanodomains, which is overdamped at all the temperatures, while the A_1 component is underdamped at all temperatures. Both soft phonons exhibit clear shifts with temperature. The E mode component exhibits softening towards $T^*=350$ K and 400 K in PMT and PMN, respectively, and hardening below this temperature (Fig. 6b).

Static permittivity $\epsilon'_{0\perp}$ calculated from the E mode contributions follows the Curie-Weiss behavior above 400 K (Fig. 1b) which corresponds to previous observations above T_d .⁹⁰ Deviation from Curie-Weiss dependence, previously observed below T_d in the low- and radio-frequency dielectric data,⁹⁰ can be explained by appearance of dielectric relaxations at lower frequencies⁸² which mask the high-frequency dielectric peak at T^* (see the EMA peak calculated using effective media approximation in Fig. 3). The E mode softening towards T^* is a hint of a local symmetry-lowering of the crystal structure within the polar nanodomains.

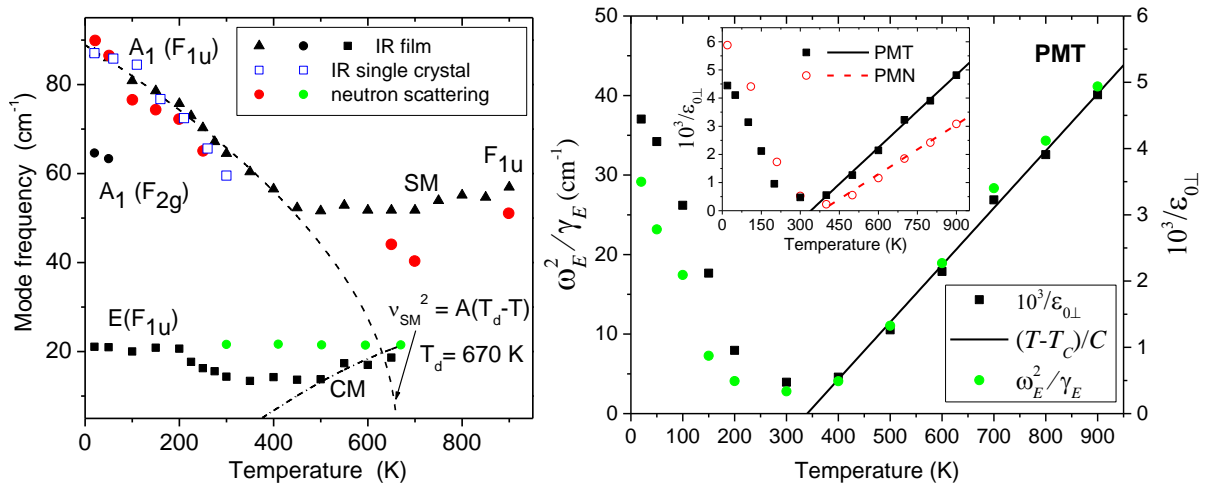


Fig. 6. Left: Temperature dependences of the polar phonon frequencies in PMN. Solid points mark data obtained on PMN thin film, open circles and squares are soft mode frequencies from inelastic neutron scattering and IR reflectivity of PMN single crystal. After Ref. 87. Right: Temperature dependence of the reciprocal static permittivity $1/\epsilon_{0\perp}$ (solid squares) obtained from the EMA fit of E -component IR and THz spectra. Solid lines are results of the Curie-Weiss fit. Solid green circles mark the overdamped E component of the soft mode frequency characterized by ω_E^2/γ_E . Inset: $1/\epsilon_{0\perp}$ of PMT compared with that of PMN. From Ref. 89.

5. Strain-induced ferroelectric phase transitions in incipient ferroelectrics

Incipient ferroelectrics are paraelectric materials exhibiting a large increase of the permittivity on cooling due to a phonon softening as follows from the Lyddane-Sachs-Teller relations. The permittivity usually saturates at low temperatures, but the FE PT does not occur due to quantum fluctuations, hence these materials are also called quantum paraelectrics. The most famous incipient ferroelectrics are SrTiO_3 and KTaO_3 and because their quantum

paraelectric phases are very sensitive on any perturbations like doping, strain or electric field, the FE phase can be easily induced in these systems.⁶⁶

Choice of the substrate is the key factor for the strain, as the lattice mismatch leads to tensile or compressive strain in thin films. In 2004 it was proved that 1 % tensile strain caused by the DyScO₃ substrate can induce a FE PT near 300 K in SrTiO₃.⁹¹ We have shown that the PT is driven by the in-plane polarized FE soft mode, i.e. it is of the displacive type.^{92,93} On the other hand, the ~1% compressive strain caused by NdGaO₃⁹⁴ or (LaAlO₃)_{0.29}-(SrAl_{1/2}Ta_{1/2}O₃)_{0.71} (LSAT)⁹⁵ substrates caused dramatic stiffening of the in-plane polarized soft-mode frequency (Fig. 9), so the FE PT cannot be revealed from the IR spectra. Nevertheless, the soft phonon polarized normal to the film plane (unfortunately, not active in near-normal IR reflectance geometry) should induce the FE PT in compressively strained SrTiO₃ grown on LSAT substrate, because the FE polarization $\mathbf{P}||c$ was revealed in second harmonic generation studies.⁹⁶ Influence of various substrates, film thicknesses, grain size and their boundaries in films and ceramics of SrTiO₃ on phonons is reviewed in Ref. ⁹⁷.

SrTiO₃ is the $n = \infty$ member of the Sr_{n+1}Ti_nO_{3n+1} homologous series. Bulk Sr_{n+1}Ti_nO_{3n+1} crystallizing in Ruddlesden-Popper structure (Fig. 10a), exhibit incipient FE behavior and their permittivity increases with the number of perovskite layers n .^{98,99} In 1% tensile strained

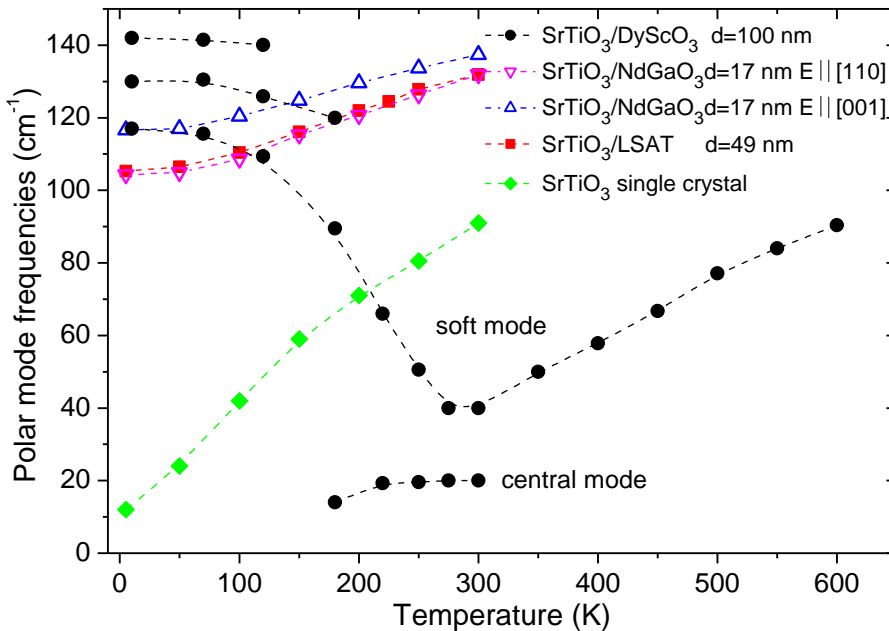


Fig. 9. Temperature dependences of the soft mode frequencies in SrTiO₃ crystal and strained films grown on various substrates. Compressively strained films grown on NdGaO₃ or LSAT substrates exhibit stiffening of the soft mode with respect to the crystal, while tensile strained SrTiO₃/DyScO₃ exhibits a soft mode anomaly and appearance of the central mode near 300 K due to a high lattice anharmonicity near strain-induced FE PT. Below ~180 K, two new modes activate above 120 cm⁻¹ in this film due to the antiferrodistortive PT within the ferroelectric phase. From Ref. 97.

$\text{Sr}_{n+1}\text{Ti}_n\text{O}_{3n+1}$ films grown on DyScO_3 , FE PTs were observed in samples with $n \geq 3$ with T_c increasing with the rising number of perovskite layers n .¹⁰⁰ THz transmission and IR reflectivity spectra reveal the FE soft mode, which drives the FE PT, but near T_c the dielectric strength of a central mode dominates.¹⁰¹ The $n = 6$ film ($\text{Sr}_7\text{Ti}_6\text{O}_{19}$) shows $T_c = 180$ K, high E -field tunability of permittivity and exceptionally low dielectric loss at 300 K which overcomes all the known tunable MW dielectrics.¹⁰⁰ Detail analysis of the MW, IR and THz spectra shows that the low room-temperature MW loss in this film has the origin in absence of the central mode at 300 K (Fig. 10b), while the high tunability of permittivity is due to sensitivity of the soft mode to the E -field.¹⁰¹ The strain quickly relaxes with increasing $\text{Sr}_{n+1}\text{Ti}_n\text{O}_{3n+1}$ film

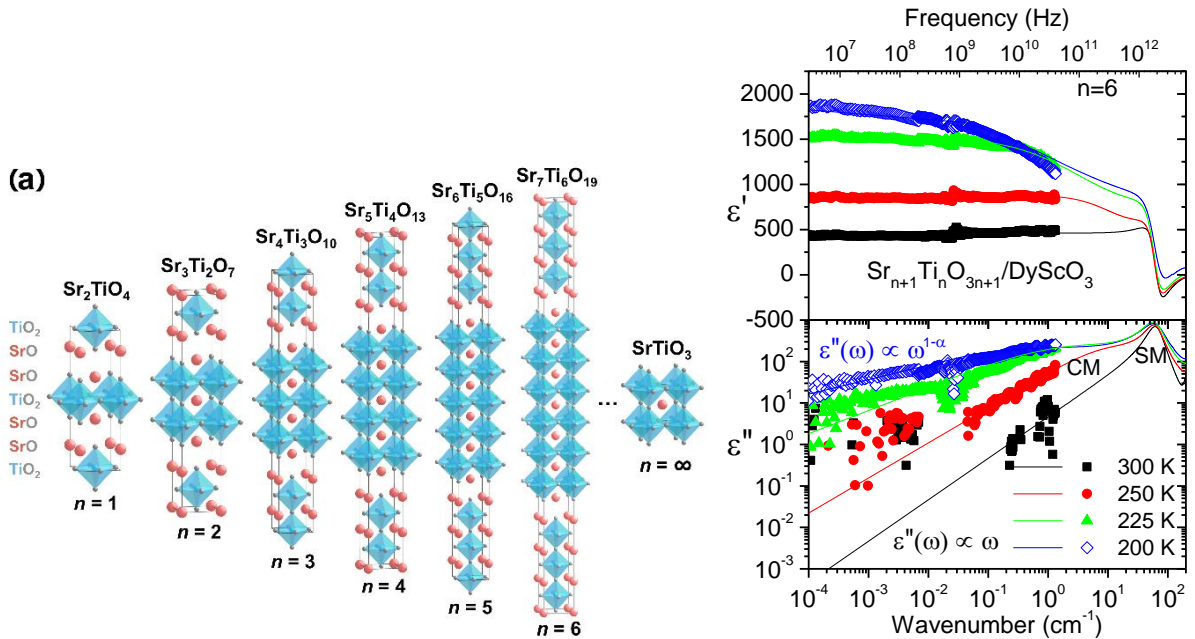


Fig. 10 a) Schematics of the crystal structure of a unit cell of the $n=1-6$ and $n=\infty$ members of the $\text{Sr}_{n+1}\text{Ti}_n\text{O}_{3n+1}$ homologous series. b) Complex dielectric spectra of a strained $\text{Sr}_7\text{Ti}_6\text{O}_{19}$ thin film measured at different temperatures. The points are experimental data between 3 MHz and 40 GHz. The curves show results of the fits to the experimental MW and far IR spectra. At room temperature the MW loss is low, because it is determined only by the phonon contributions (Eq. 2), while at lower temperatures a dielectric relaxation (central mode) enhances the MW loss. From Ref. 101.

thickness, which limits its application. Recently, it was proved that if one SrTiO_3 layer in $\text{Sr}_{n+1}\text{Ti}_n\text{O}_{3n+1}$ is replaced by BaTiO_3 , the chemical pressure reduces the strain, thicker films can be grown and simultaneously excellent MW properties are kept.¹⁰² Today's best room-temperature MW tunable dielectric parameters were achieved in films of $\text{Sr}_6\text{BaTi}_6\text{O}_{19}$, where unprecedented low loss at frequencies up to 125 GHz was observed.¹⁰² This makes this film very attractive for high-frequency applications in 5G telecommunications.

The second most popular incipient FE is KTaO_3 , where only two publications were devoted to the IR and THz SM studies,^{103,104} but the soft mode was also studied in details using the hyper-Raman scattering.²⁴ In Ref. 104 the chemical solution deposited polycrystalline (grain size ~ 160 nm) film ($d \approx 200$ nm) on (0001) sapphire substrate, partially (001) oriented, was shown to be FE with a diffuse $T_C \approx 60$ K. The reason for it was shown to be the compressive strain due to larger thermal expansion of the sapphire compared to KTaO_3 (the film was annealed at 900°C), which could induce a FE phase with preferential out-of-plane orientation of P_s . In spite of it a minimum in the frequency of the in-plane polarized soft mode was observed near T_C ,¹⁰⁴ while in crystal and ceramics the soft mode gradually softens on cooling and levels off at ~ 20 cm^{-1} below 20 K.^{24,105}

6. Soft-mode spectroscopy in multiferroics with displacive ferroelectric phase transitions

Multiferroics are materials exhibiting magnetic and FE order simultaneously. Since the magnetization can be controlled by the electric field (i.e. magnetoelectric effect) in these materials, they have high promising potential for applications in spintronics and nonvolatile memories and therefore they are intensively studied. In this chapter we will focus on type-I multiferroics, where FE and magnetic phases appear independently and therefore their magnetoelectric coupling is relatively small.

The most studied multiferroic is BiFeO_3 , because it is one of the few single-phase room-temperature multiferroic with high FE $T_C = 1120$ K and antiferromagnetic Néel temperature $T_N = 643$ K. Unfortunately, its magnetoelectric coupling is weak and the 1.2 % change of its permittivity with magnetic field (magnetodielectric effect) observed above 200 K is mainly caused by a combination of magnetoresistance influencing related Maxwell-Wagner dielectric relaxation in electrically leaky samples.¹⁰⁶ In the insulating phase (i.e. below 200 K) the magnetodielectric effect drops down below 0.3 % in the magnetic field 9 T. The effect is small because the linear magnetoelectric effect is forbidden in incommensurately modulated cycloidal magnetic structure. Only above 19 T the antiferromagnetic structure becomes unmodulated and the linear magnetoelectric effect is allowed.¹⁰⁷

IR reflectivity and THz transmission spectra revealed 13 polar phonons which exactly correspond to the rhombohedral $R3c$ symmetry.¹⁰⁶ On heating, the phonons broaden and gradually merge in three bands allowed in the cubic perovskite $Pm\bar{3}m$ structure expected in the paraelectric phase. We measured the spectra up to 900 K and found an optical soft mode, which is responsible for an increase of the low-frequency permittivity with rising temperature (Fig. 11

left). Phonon softening is only partial, suggesting that the phase transition into the paraelectric phase will be of the first order.¹⁰⁶ Experimental data near T_c are missing in literature, but our conclusion is consistent with the theoretical prediction¹⁰⁸ of the first-order PT into intermediate antiferrodistortive tetragonal phase $I4/mcm$ (1100 – 1450 K) and the cubic $Pm\bar{3}m$ phase should be energetically stable only above 1450 K, which is temperature, where the BiFeO_3 decomposes.

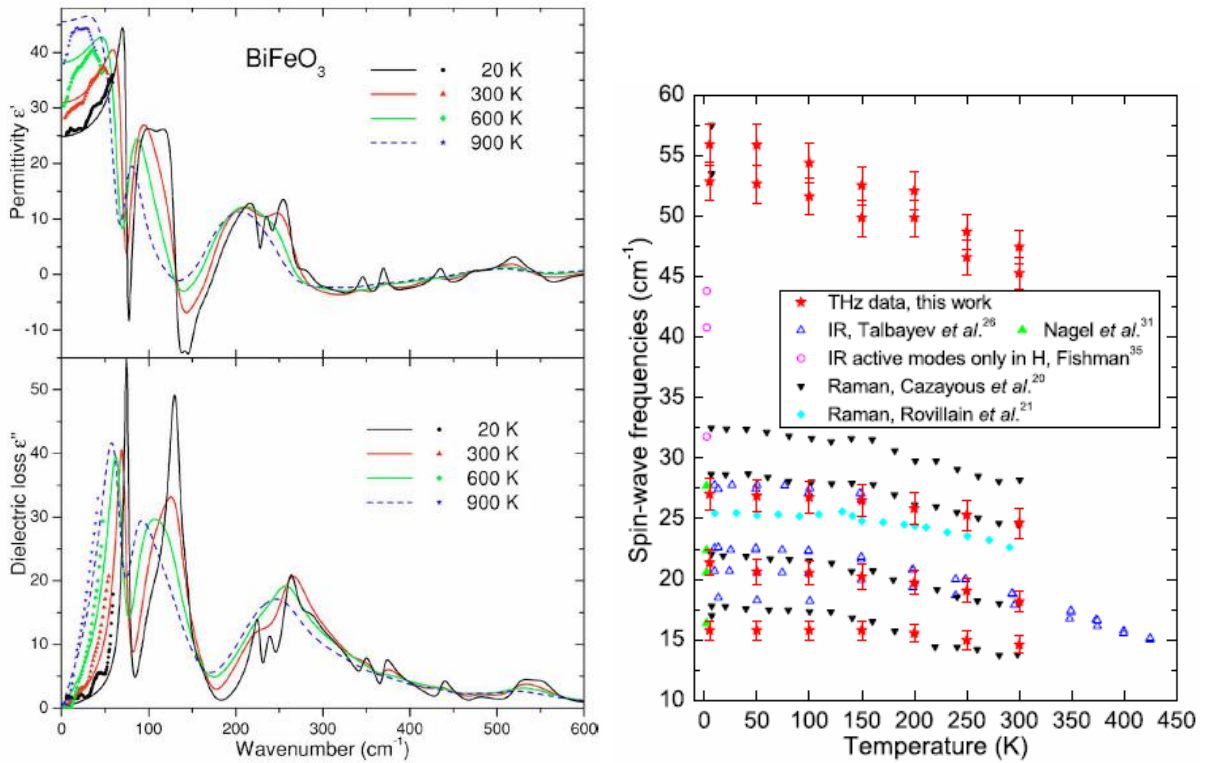


Fig. 11 Left: Complex dielectric spectra of BiFeO_3 ceramics at selected temperatures. The dots are experimental THz data; lines are results of the IR reflectivity fits. Note the shifts of ϵ'' peaks to lower frequencies due to the phonon softening on heating (from Ref. 106). Right: Temperature dependence of the electromagnon frequencies in BiFeO_3 determined from the fits of our THz spectra compared with published frequencies obtained from Raman scattering and far IR spectra (from Ref. 109).

THz and Raman spectra revealed number of spin excitations, whose frequencies soften towards T_N (see Fig. 11 right).¹⁰⁹ These magnons are electrically and magnetically active,¹¹⁰ therefore can be called electromagnons and are activated in the spectra from outside of the Brillouin zone center due to the incommensurate modulation of spins in the antiferromagnetic phase.¹¹¹

Fennie and Rabe¹¹² suggested theoretically a new route for preparation of multiferroics with a strong magnetoelectric coupling. They proposed to use a biaxial strain in epitaxial thin films for inducing the FE and ferromagnetic states in materials, which are in the bulk form paraelectric and antiferromagnetic. The basic condition for such materials is the strong spin-

phonon coupling. Based on their first-principles calculations, Fennie and Rabe¹¹² proposed to use EuTiO₃, because this material is in its bulk form an incipient FE and its permittivity strongly changes at the antiferromagnetic PT due to the strong spin-phonon coupling.¹¹³ Temperature dependence of the permittivity in EuTiO₃ crystal was successfully explained by strongly anharmonic behavior of the soft mode.^{114,115} The bulk EuTiO₃ ceramics undergoes an antiferrodistortive PT from the high-temperature cubic $Pm\bar{3}m$ ($Z=1$) structure to the tetragonal $I4/mcm$ ($Z=1$) phase near 280 K.^{116,117} For that reason the soft mode splits in the tetragonal phase and both components of the soft mode soften on cooling. Lee *et al.*¹¹⁸ grew the epitaxial EuTiO₃ thin films on DyScO₃ substrates and due to the 1% tensile strain the soft mode (seen in the IR reflectance) is much softer than in the bulk, reaching a minimum frequency at $T_c = 250$ K (Fig. 12a). Due to the soft mode anomaly, the permittivity exhibits a maximum (Fig. 12b), typical for the displacive FE PTs. FE polarization was calculated from the first principles¹¹⁸ and also estimated based on the value of T_c ¹¹⁹ with the resulting value 20 – 30 $\mu\text{C}/\text{cm}^2$. The non-centrosymmetric structure of the thin film has been also proven by observation of the second harmonic generation signal below T_c . Magneto-optic Kerr effect studies revealed strain-induced ferromagnetic state below 4.3 K. All these studies confirmed theoretical predictions that the strain can induce FE and ferromagnetic order in paraelectric antiferromagnets. Nevertheless, the magnetic Curie temperature $T_c = 4.3$ K is too low for practical applications, despite of the FE critical temperature close to room temperature which can be even enhanced by a higher strain.

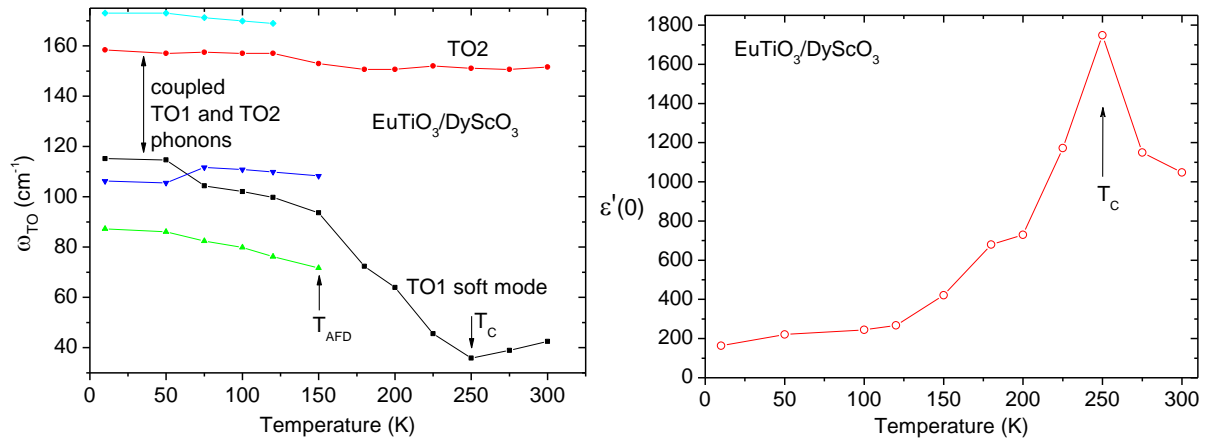


Fig. 12 (a) Temperature dependence of the lowest-frequency phonons and (b) static phonon permittivity in the EuTiO₃ film grown on DyScO₃. Soft mode anomaly induces dielectric anomaly at T_c and two new modes activate in the IR spectra below 150 K due to an antiferrodistortive PT at T_{AFD} . Modified after Ref. 118.

Permittivity in EuTiO₃ dramatically changes with the magnetic field.¹¹³ Since the high value of permittivity is caused by the soft mode contribution, it is natural to expect that the soft mode

frequency will change with the magnetic field. First attempt to see the soft mode tuning in magnetic field in ceramics was not successful due to too broad reflectivity band.¹¹⁴ Nevertheless, in compressively strained EuTiO_3 films grown on LSAT substrates the soft phonon is significantly stiffened above 100 cm^{-1} and shows a rather narrow reflectance peak, whose change with magnetic field and temperature can be studied with much higher accuracy than in the bulk samples.¹²⁰ Actually, reliable tuning of the soft mode frequency by 2 cm^{-1} was detected in the IR reflectance spectra,¹²⁰ explaining in this way the magnetodielectric effect in EuTiO_3 .

A FE PT can be induced also in $(\text{Eu}_{1-x}\text{Ba}_x)\text{TiO}_3$ solid solution.¹²¹ $(\text{Eu}_{0.5}\text{Ba}_{0.5})\text{TiO}_3$ and $(\text{Eu}_{0.5}\text{Ba}_{0.25}\text{Sr}_{0.25})\text{TiO}_3$ exhibit displacive FE PTs at 215 and 130 K, respectively, because the FE soft modes were observed in THz and IR spectra.^{122,123} In both materials, the Néel temperature remains close below 2 K. Since T_N is very low and internal electric field is of order of 10 MV/cm in the FE phase and this field (and the FE polarization) can be switched at low temperatures by an external electric field of 3-10 kV/cm⁻¹, the system was suggested for measurement of an electron dipole moment, which could be revealed in observation of the linear magnetoelectric effect in the paramagnetic state.¹²¹ This effect is forbidden in the paraelectric state, but if the linear magnetoelectric effect would be observed, it could be explained by a non-zero electron dipole moment which violates both space-inversion and time-reversal symmetry. These are basic conditions for the linear magnetoelectric effect. A change of magnetization with electric field was really observed in $(\text{Eu}_{0.5}\text{Ba}_{0.5})\text{TiO}_3$ at 4 K,¹²⁴ but since the sample heats in the field above the coercive field 10 kV/cm, the effect could be explained by a temperature change. Nevertheless, the measurement allowed to determine that the electron dipole moment should be smaller than $6 \times 10^{-25} \text{ ecm}$ (e marks a charge of electrons).¹²⁴ $(\text{Eu}_{0.5}\text{Ba}_{0.25}\text{Sr}_{0.25})\text{TiO}_3$ could be more suitable for such studies, because its coercive field is three times lower so that the sample heating could be smaller.¹²³

Ten years ago, Bousquet et al. used density functional theory and predicted a strain-induced displacive FE PT in the ferromagnetic EuO , but since its optical phonon is highly stable, the critical strain was predicted to be around 4%. Group of D. Schlom from Cornell University began growing strained EuO thin films using molecular-beam epitaxy on various substrates to impose epitaxial strain and we investigated the phonon properties of the strained EuO films using the IR reflectance spectroscopy. We found that although the phonon frequency decreased with tensile strain as predicted, the previously predicted critical 4% tensile strain was insufficient to induce a FE phonon instability.¹²⁶ Hearing this news, our theory colleagues from Belgium performed new calculations using a more advanced hybrid functional and found that

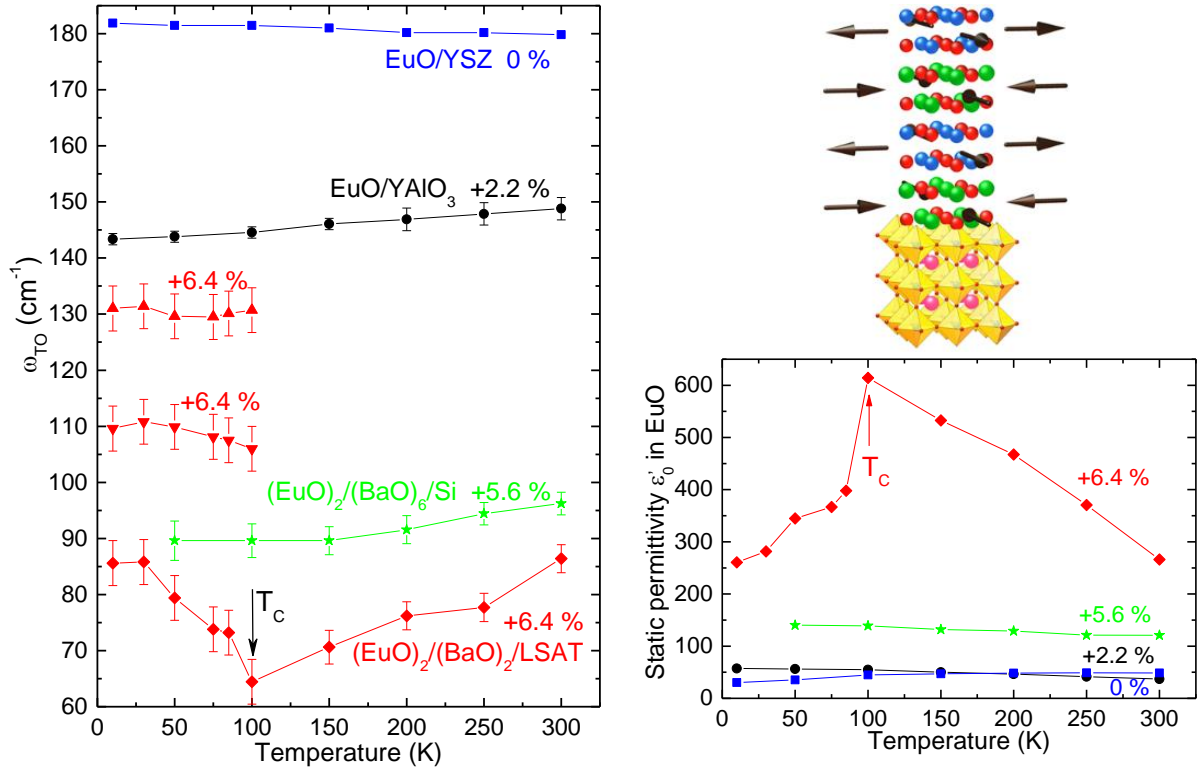


Fig. 13. a) Temperature dependence of the EuO optical phonon frequency in epitaxial (001)-oriented EuO films with various nominal strain levels imposed by underlying (001) YSZ, (110) YAlO₃, (001) Si and (001) LSAT substrates. +5.6% and +6.4% nominal tensile strain was reached in [(EuO)₂/(BaO)₆]₂₈/Si and [(EuO)₂/(BaO)₂]₃₅/LSAT superlattices, respectively. The EuO phonon in the superlattice with the highest strain (+6.4%) exhibits softening typical for a displacive FE PT. Upon undergoing the PT, the single optical phonon splits into three phonons due to the reduction of the symmetry of the (EuO)₂ unit cell that occurs below T_C . b) Schematic illustration of crystal structure of the (EuO)₂/(BaO)₂ superlattice on an (001) LSAT perovskite substrate in which the (EuO)₂ layer is under biaxial tension and the (BaO)₂ layer is under biaxial compression. The directions of both strains are marked by arrows. Eu, Ba and O atoms are shown in blue, green and red, respectively. c) Temperature and strain dependence of the static relative permittivity of the EuO films and EuO layers in the (EuO)_x/(BaO)_y superlattices. The permittivity values were calculated from fits of the IR reflectance. The FE critical temperature observed for the [(EuO)₂/(BaO)₂]₃₅ superlattice strained to LSAT is marked by the arrow. From Ref. 126.

more than 5.8% tensile strain is required for the phonon instability and resulting FE state. Biaxially straining EuO more than 5% is challenging, as such films tend to relax after the epitaxial growth of only a few monolayers. We overcame this challenge by growing superlattices made of EuO and BaO. The latter material has a larger lattice parameter than EuO and therefore helps to maintain the tensile strain in the EuO thin layers. In (EuO)₂/(BaO)₂ superlattices grown epitaxially on LSAT substrates we achieved 6.4% biaxial tensile strain in the EuO layers and observed a FE soft mode anomaly at 100 K, which induces a peak in the dielectric permittivity typical of a FE PT (see Fig. 13b). Magnetic measurements simultaneously proved that the superlattices remain ferromagnetic, i.e. they are multiferroic.¹²⁶

High ferromagnetic and FE critical temperatures were theoretically predicted in the strained SrMnO_3 thin films.¹²⁷ The prediction was supported by extremely strong spin-phonon coupling in this material, which we observed near T_N in the IR spectra of SrMnO_3 ceramics.¹²⁸ The film with 1.7% tensile strain grown on LSAT substrate exhibited FE $T_c \approx 400$ K and Néel temperature $T_N < 200$ K.¹²⁹ Nevertheless, these films were too conducting, which did not allow to study the magnetoelectric coupling. Since the FE PT should be of displacive type, we investigated the IR spectra of several strained SrMnO_3 thin films, but did not obtain reliable phonon parameters, presumably due to the high phonon damping in this material. Ba substitution of Sr induces negative chemical pressure in the lattice and therefore the FE PT was observed in $\text{Sr}_{1-x}\text{Ba}_x\text{MnO}_3$ crystals¹³⁰ and ceramics¹³¹ near 350 K. The soft mode exhibits minimum at this temperature¹³² and splits in the FE phase due to change of symmetry from cubic to tetragonal phase.¹³¹ Both modes exhibit also other anomalies at T_N due to the strong spin-phonon coupling (Fig. 14).

Many type-I multiferroics exhibit improper FE PT connected with a multiplication of unit cell below T_c . YMnO_3 ¹³³ and also the famous BiFeO_3 ¹⁰⁸ belong to this family. We investigated a two-layered BaMnO_3 , which at high temperatures crystallizes in nonpolar hexagonal $P6_3/mmc$ structure and its unit cell triples below $T_C = 130$ K and the space group changes to $P6_3cm$.¹³⁴

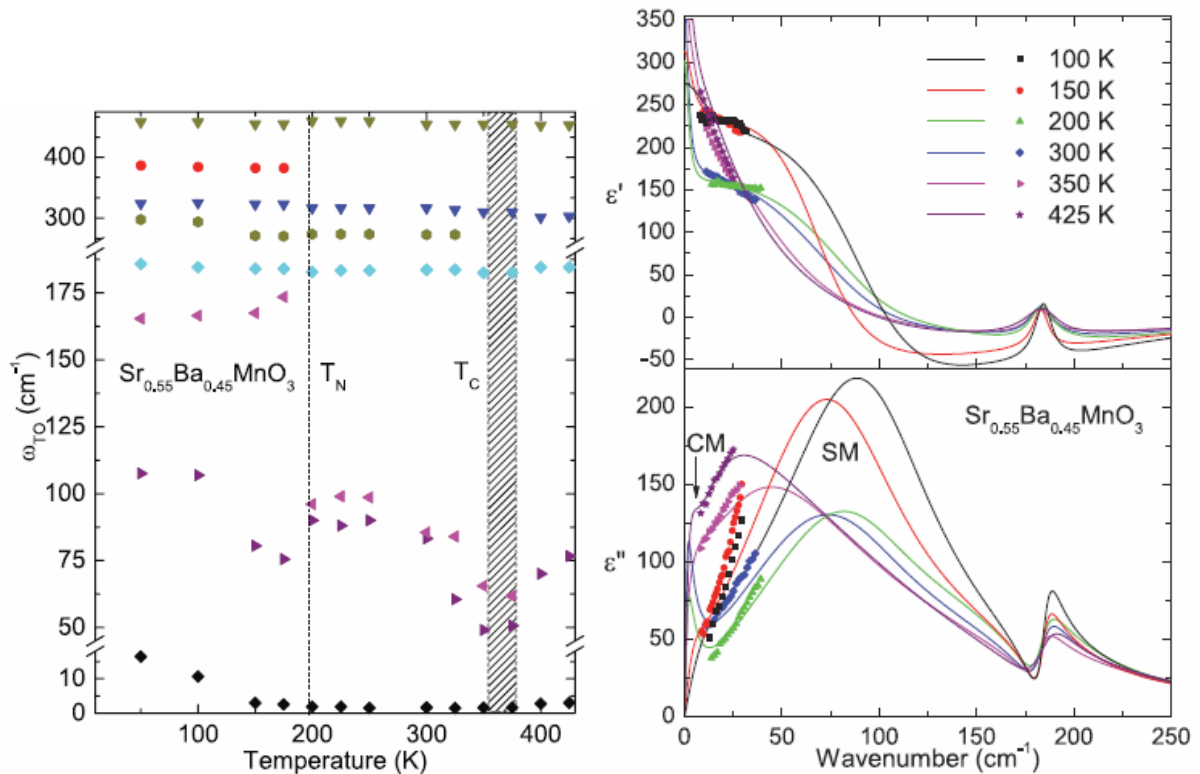


Fig. 14. Left: Temperature dependence of the phonon frequencies in $\text{Sr}_{0.55}\text{Ba}_{0.45}\text{MnO}_3$ ceramics obtained from the fits of IR and THz spectra. The area corresponding to T_c is hatched. Note the soft mode minimum near T_c and anomalies of the two soft mode components near T_N . Right: Complex dielectric spectra obtained from the fits of IR reflectivity and THz permittivity spectra at various temperatures. The experimental THz data are marked by dots. After Ref. 131.

Unlike in all proper ferroelectrics, where a peak in $\epsilon'(T)$ is seen at T_C , only change of slope in $\epsilon'(T)$ was observed at T_C (Fig. 15c), because the PT is driven by a soft Brillouin zone-boundary phonon of K_3 symmetry with a wavevector $\mathbf{q} = (1/3, 1/3, 0)$. This IR inactive phonon is coupled with the hard zone-center Γ_2^- mode. Owing to the Brillouin-zone folding below T_C , the soft mode becomes a zone-center mode in the FE phase, which activates in the IR and Raman spectra and hardens on cooling. This phonon has a small dielectric strength, so it only partially explains the increase in ϵ' below T_C (Fig. 15).¹³⁴ An additional dielectric relaxation, observed in the MW region, is probably due to the vibration of the FE domain walls. On cooling, this temperature-activated process slows down and the distribution of relaxation frequencies of domain wall vibration broadens. This explains the relaxor-like dielectric dispersion seen below 70 K. Contribution of domain wall motion in ϵ' reduces under the bias electric field (Fig. 15 left) because the FE domain size increases and domain wall concentration reduces under the field. An antiferromagnetic order appears at 53 K, but short-range magnetic correlations were

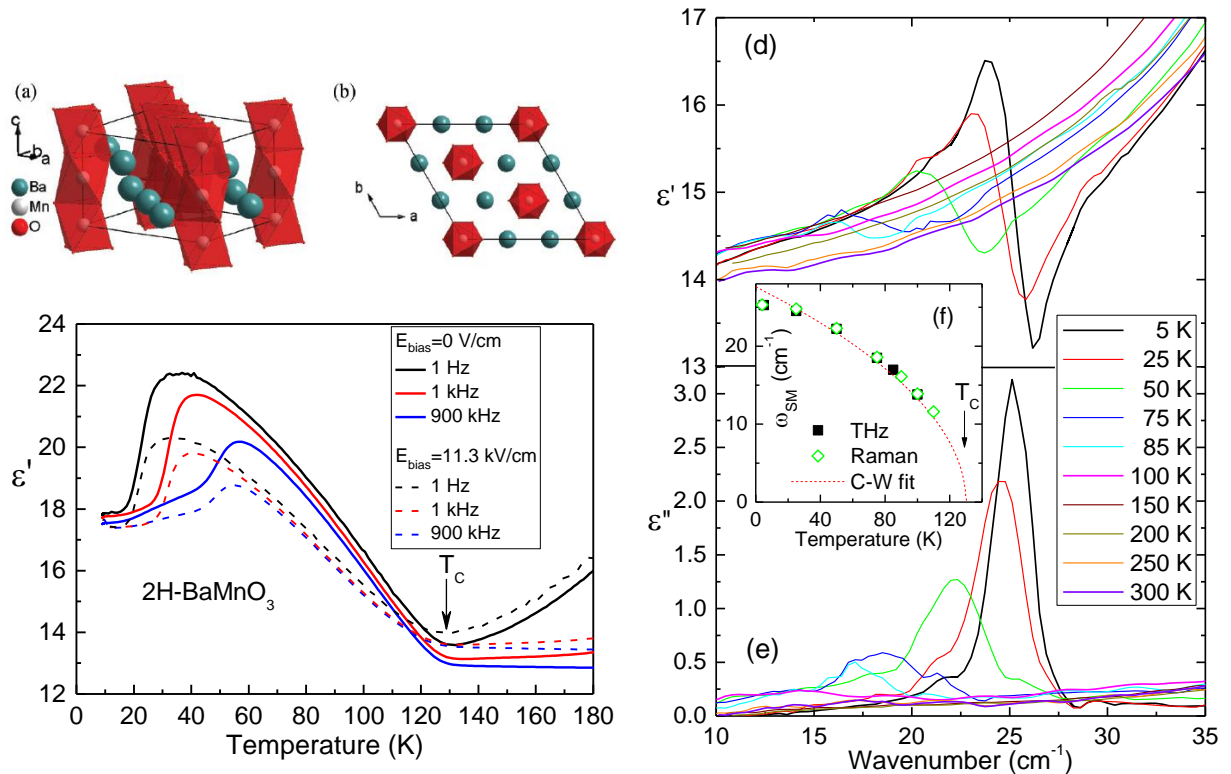


Fig. 15 Low-temperature crystallographic structure of 2H-BaMnO₃ featuring face-sharing MnO₆ octahedrons (space group $P6_3cm$) from a) side view and b) top view (from Ref. 135). c) Temperature dependence of dielectric permittivity of 2H-BaMnO₃ ceramics measured at various frequencies and in or without bias electric field. d) Real and e) imaginary parts of complex THz dielectric permittivity showing activation and hardening of a new soft phonon below $T_C = 130$ K. f) Temperature dependence of the soft mode frequency obtained from the THz and Raman spectra. Dashed line is the result of the fit using the Cochran law.

observed in the EPR spectra up to 230 K.¹³⁴

7. Spin-induced multiferroics

In 2003, a new class of multiferroics was discovered in TbMnO₃. Kimura et al.¹³⁶ observed a narrow and small peak in $\varepsilon'(T)$ at the temperature, where the cycloidal magnetic structure of TbMnO₃ changes its modulation. Its FE polarization was 3 or 4 orders of magnitudes lower than in classical ferroelectrics, but since the polarization direction was possible to control by the direction of external magnetic field, the authors explained it as caused by the spin interactions. Due to this fact the polarization is more sensitive to magnetic field and the magnetoelectric coupling is huge. Shortly after this observation, many new spin-induced ferroelectrics were discovered, called now type-II multiferroics.¹³⁷ Since the order parameter of the FE PT transition is not polarization, these multiferroics belong to improper or pseudoproper ferroelectrics.¹³⁸ For that reason, one cannot expect FE soft phonons or critical dielectric relaxation in these materials and therefore the dielectric anomalies are small at T_C . Nevertheless, in one paper a critical relaxation in multiferroic MnWO₄ was reported, but it was observed in the MW region only less than 1 K above the T_C .¹³⁹ This soft dielectric excitation was explained by an electromagnon¹³⁹ coupled with the polar phonon. Just this excitation, activated in the dielectric spectra in a close proximity to the FE PT, is responsible for the tiny dielectric anomaly at T_C in MnWO₄ and most probably also in other spin-induced ferroelectrics.

The electromagnons (i.e. electrically active magnons) were first time discovered by Pimenov *et al.* in THz spectra of TbMnO₃ and DyMnO₃¹⁴⁰ and since that time they were observed in many multiferroics.¹³⁷ Characteristic feature of the electromagnon is its activity in the dielectric THz or MW spectra and its coupling with polar phonons. It means, it receives its dielectric strength from the IR active phonons. Due to off-diagonal dynamic magnetoelectric coupling, THz or MW absorption of electromagnons exhibits a directional dichroism, i.e. the absorption depends on propagation direction of the electromagnetic radiation.¹³⁷ We have observed electromagnons in ε phase of Fe₂O₃,¹⁴¹ Ni₃TeO₆,¹⁴² Ni_{3-x}Co_xTeO₆,¹⁴³ quadruple perovskites CaMn₇O₁₂¹⁴⁴ and SrMn₇O₁₂,¹⁴⁵ Y-type hexaferrite BaSrCoZnFe₁₁AlO₂₂¹⁴⁶ and Z-type hexaferrite (Ba_xSr_{1-x})₃Co₂Fe₂₄O₄₁.¹⁴⁷

Interestingly, the Y-type hexaferrite exhibits an asymmetric change in static FE polarization P with magnetic field H ($P(H) = -P(-H)$) whereas the Z-type hexaferrite shows a symmetric change ($P(H)=P(-H)$). These facts were clarified recently: the static magnetoelectric coupling in Y-type hexaferrites can be explained only by the inverse Dzyaloshinskii-Moriya interaction

while additional p - d hybridization becomes dominant in the Z-type hexaferrite.¹⁴⁸ The magnetoelectric coupling is giant^{149,150} because the magnetic structures of hexaferrites are extremely sensitive to external magnetic field. THz and Raman spectroscopic studies of Y- and Z-type hexaferrites revealed the electromagnons in both kinds of the spectra.^{146,147,151,152} It is plausible because all polar excitations should be both IR and Raman active in non-centrosymmetric FE phase. Our analytical calculations confirm that the electromagnons are activated by the exchange striction.¹⁴⁶ Also, we were able to determine selection rules for electromagnons in various magnetic structures of hexaferrites. Fig. 16 shows that the electromagnon in Y-type hexaferrite softens on heating towards the magnetic (and simultaneously FE) PT near room temperature so that it behaves similarly as the FE soft phonon in displacive ferroelectrics. Since the electromagnon is activated in the THz and Raman spectra only in alternating longitudinal conical magnetic structure and this structure disappears in the magnetic fields above 4 T, intensity of the electromagnon weakens and its frequency softens with magnetic field and finally this excitation disappears in the field above 4 T (Fig. 16b). On the other hand, a new excitation appears in the THz spectra below 0.4 THz in the field above 4 T. This is a ferromagnetic resonance (FMR), which linearly shifts from MW to THz region with rising magnetic field.¹⁴⁶

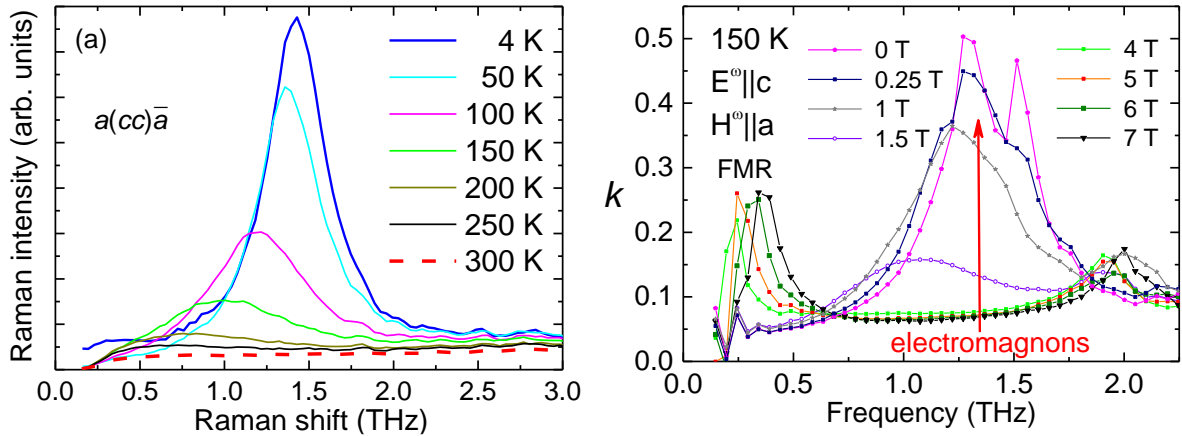


Fig. 16. (a) Temperature dependence of the Raman scattering spectra showing the electromagnon in the Y-type hexaferrite BaSrZnCoFe₁₁AlO₂₂. (b) Magnetic field dependence of the extinction coefficient of the Y-type hexaferrite in the THz region measured at 150 K. In the field above 4 T, the electromagnon doublet disappears and a ferromagnetic resonance (FMR) appears in the low-frequency part of the spectra. Modified from Ref. 146.

Recent MW studies of the magnetic permeability revealed the FMR in the Z-type hexaferrite (Ba_xSr_{1-x})₃Co₂Fe₂₄O₄₁ at frequencies below 2 GHz (measured without magnetic field).¹⁵³ Its frequency showed a linear decrease on heating towards the magnetic PT temperature 500 K, where the magnetic structure changes from conical to collinear. FMR studies performed near 9

GHz with a magnetic field up to 10 kOe also confirmed the PT near 500 K. Moreover, FMR spectra were tunable by an external dc and ac electric field which allowed to determine the value of magnetoelectric coefficient $\alpha_E = 390$ ps/m at 170 K.¹⁵³ The value of α_E was one order of magnitude lower than that reported at 10 K,¹⁵⁰ but still one or even four orders of magnitude higher than in other “high-temperature” multiferroics. Sensitivity of the FMR on electric field gives an evidence that the FMR has an electromagnon character.

In 2012, an unusually strong spin-order induced FE polarization was revealed in $\text{CaMn}_7\text{O}_{12}$ below 90 K. Subsequently it was shown that the quadruple perovskites $(\text{AMn}_3)\text{Mn}_4\text{O}_{12}$ ($A^{2+} = \text{Cd, Sr, Pb}$) exhibit a similar sequence of structural PTs:^{154-155,156} Near 400 K, they undergo

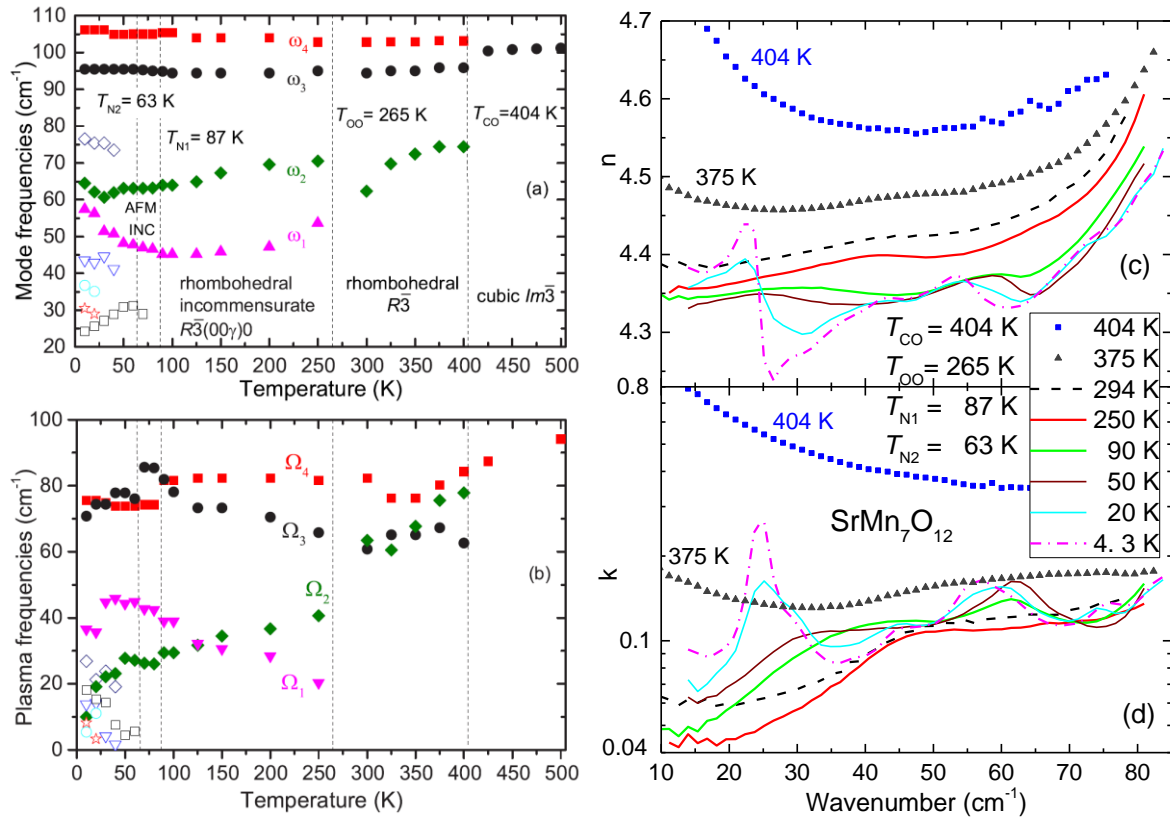


Fig. 17. Temperature dependence of (a) the low-frequency excitations and (b) their plasma frequencies $\Omega_j = \sqrt{\Delta\epsilon_j}\omega_j$ observed in the THz and IR spectra of $\text{SrMn}_7\text{O}_{12}$. The open symbols correspond to spin excitations or phonons activated by breaking of the inversion center, whereas the remaining phonons are marked by solid symbols. (c) Real and (d) imaginary parts of the complex refractive index of $\text{SrMn}_7\text{O}_{12}$ ceramics obtained from the THz time-domain spectroscopy. From Ref. 145.

a charge-ordering metal-insulator PT from a cubic to a rhombohedral $R\bar{3}$ structure. The next PT gives rise to the Mn orbital ordering and an incommensurate structural modulation along the c axis below ca. 250 K. On further cooling, the samples show two magnetic PTs near 90 K and 40 K with PT temperatures depending on the chemical composition. The antiferromagnetic

phases are helical and incommensurately modulated. We investigated IR, THz and Raman response of AMn_7O_{12} ($A=Ca, Sr$) ceramics and found similar dramatic changes in phonon spectra reflecting changes in phonon selection rules in various crystal structures (Fig 17) including new phonons appearing in the spin-order-induced FE phases.^{144,145} The strongest variations occur in THz spectra near the two magnetic PTs (see Fig. 17c,d). They activate new modes in the spectra, with resonance frequencies and intensities changing with temperature and magnetic field. Below the lowest-temperature magnetic PT, we observed a transfer of plasma frequencies Ω_1 and Ω_2 (defined as a square roots of oscillator strength) from the low-frequency phonons to these excitations, therefore we assigned them to electromagnons, because they must be polar.

8. Resume

In this review, a basic concept of the FE soft modes driving the FE PTs is explained and demonstrated in materials which I investigated within the last 25 years. In Rochelle salt – the first know FE crystal – we show that although this material was for long time considered as a typical example of the system with an order-disorder PT, two coupled polar phonons show anomalous softening with rising temperature and these phonons are coupled with the MW dielectric relaxation so that this system belongs to crossover between order-disorder and displacive type of the PT.³⁰ On the other hand, another related tartate - lithium thallium tartrate monohydrate – shows a typical behavior of the displacive ferroelectrics.⁵² Lead-based relaxor ferroelectrics with perovskite structure show a strong and soft dielectric relaxation whose distribution of relaxation frequencies anomalously broadens on cooling towards the freezing temperatures and covers the frequencies from sub-Hz up to THz region even below the freezing temperatures.^{75,79} Although the relaxors are cubic in the whole temperature interval, the phonons are split at all temperatures due to locally broken center of symmetry in polar nanodomains and the lowest frequency phonon undergoes a critical softening towards $T^* = 350 - 400$ K, giving evidence about a local PT in polar nanodomains.^{82,89} In incipient FE $SrTiO_3$, $Sr_{n+1}Ti_nO_{3n+1}$ and $KTaO_3$, frequencies of the soft phonons strongly reduce on cooling and saturate near liquid helium temperatures due to quantum fluctuations, but we have shown that the epitaxial strain can induce displacive FE PTs, which can be revealed in the phonon behavior.^{92,94,100,101,104} In antiferromagnetic and incipient ferroelectric $EuTiO_3$, 1% tensile strain induces not only a displacive FE PT at 250 K, but the antiferromagnetic structure changes also to ferromagnetic one due a strong spin-phonon coupling.¹¹⁸ In ferromagnetic EuO , a huge tensile strain (more than 6%) was able to induce a displacive FE PT,¹²⁶ even if the phonon is

highly temperature stable in the bulk EuO. Incomplete phonon softening was observed in the multiferroic BiFeO₃ connected with the first-order and improper FE PT at 1100 K.¹⁰⁶ Displacive character of the FE PT was revealed in the multiferroic Sr_{0.55}Ba_{0.45}MnO₃.¹³¹ The soft mode exhibits also a strong anomaly at the antiferromagnetic PT due to a large spin-phonon coupling in this material.¹³¹ In multiferroic hexagonal BaMnO₃, the FE soft mode was observed in the THz and Raman spectra but only below $T_c=130$ K, because the improper FE PT related with a tripling of the unit cell occurs below T_c so that the soft mode has a wave vector from the Brillouin zone boundary in the paraelectric phase and therefore cannot be IR/Raman active above T_c .¹³⁴ Electromagnons were detected in the THz and Raman spectra of the multiferroic BiFeO₃,^{109,110} but also in spin-induced multiferroics with the Y- and Z-hexaferrite crystal structures,^{146,147} as well as in quadruple perovskite SrMn₇O₁₂.¹⁴⁵ Their frequencies soften on heating towards the temperatures of the magnetic PTs similarly to the soft phonons in ferroelectrics. In hexaferrites, the magnetic structures are highly sensitive to magnetic field, therefore the electromagnons disappear from the spectra at higher magnetic fields.^{146,147}

All these results demonstrate high ability and sensitivity of IR and THz spectroscopy for determining the type of FE PTs in various materials not only in the bulk form, but also in the ultrathin films, which can be highly strained and exhibit a behavior completely different from the bulk samples.

9. References

(References marked in red are attached to this thesis. Applicant is co-author of the other references marked in blue.)

-
- ¹ W. Cochran. Crystal Stability and the Theory of Ferroelectricity. *Phys. Rev. Lett.* **3**, 412-414 (1959).
 - ² W. Cochran. Crystal stability and the theory of ferroelectricity. *Advances in Physics* **9**, 387-423 (1960).
 - ³ W. Cochran. Crystal stability and the theory of ferroelectricity part II. Piezoelectric crystals. *Advances in Physics* **10**, 401-420 (1961).
 - ⁴ P.W. Anderson, Qualitative description of the phase transition in BaTiO₃-type ferroelectrics. In: Fizika Dielektrikov, Ed. By G.I. Skanavi, Moscow: Acad. Nauk USSR, 1960.
 - ⁵ V.L. Ginzburg, O polarizatsii i piezoefekte titanata bariya vblizi tochki segnetoelektricheskogo perekhoda" *JETP*, **19**, 36-41 (1949).
 - ⁶ V.L. Ginzburg, Teoria segnetoelektricheskikh javlenij, *Uspekhi Fiz. Nauk*, **38**, 490-525 (1949)
 - ⁷ V. L. Ginzburg. Phase Transitions in Ferroelectrics (Some Historical Remarks). *Ferroelectrics* **267**, 23-32 (2010).
 - ⁸ G.S. Landsberg and L.I. Mandelstam, *Z. Phys.* **58**, 250 (1920) and *Z. Phys.* **60**, 364-375 (1930)
 - ⁹ A. S. Barker and M. Tinkham. Far-Infrared Ferroelectric Vibration Mode in SrTiO₃. *Physical Review* **125**, 1527-1530 (1962).
 - ¹⁰ R. A. Cowley. Temperature Dependence of a Transverse Optic Mode in Strontium Titanate. *Phys Rev Lett* **9**, 159-161 (1962).
 - ¹¹ J. F. Scott. Soft-mode spectroscopy: Experimental studies of structural phase transitions. *Reviews of Modern Physics* **46**, 83-128 (1974).

-
- ¹² J. Petzelt, G. V. Kozlov, and A. A. Volkov. Dielectric-spectroscopy of paraelectric soft modes. *Ferroelectrics* **73**, 101-123 (1987).
- ¹³ M. E. Lines and A. M. Glass, *Principles and applications of ferroelectrics and related materials* (Clarendon Press, Oxford 1977).
- ¹⁴ S. Kamba, J. Petzelt, and V. Zelezny. Infrared reflectivity of BaMnF₄. *Czechoslovak J. Phys.* **36**, 848-854 (1986).
- ¹⁵ S. Kamba, J. Petzelt, S. P. Lebedev, V. A.A., A. Fuith, and H. Warhanek. Far infrared spectroscopy of the phase transition in KSCN. *Ferroelectrics* **109**, 3-8 (1990).
- ¹⁶ S. Kamba, J. Petzelt, V. Dvořák, Y. Goncharov, A. A. Volkov, G. V. Kozlov, and J. Albers. Far infrared spectroscopy of the phase-transition sequence in BCCD. *Ferroelectrics* **105**, 351-356 (1990).
- ¹⁷ R. Currat, J. Legrand, S. Kamba, J. Petzelt, V. Dvorak, and J. Albers. Inelastic neutron scattering study of the soft phonon branch in deuterated BCCD. *Solid State Communications* **75**, 545-549 (1990).
- ¹⁸ J. Petzelt, S. Kamba, S. Pacesova, E. Pollert, J. Sramek, O. Smrckova, and D. Sykorova. Infrared reflectivity of high-Tc YBa₂Cu₃O_{7-x} and related ceramics. *Physica Status Solidi B-Basic Research* **146**, 743-755 (1988).
- ¹⁹ S. Kamba, J. Petzelt, V. Zelezny, E. Pechen, S. Krasnosvobodtsev, and B. Gorshunov. Infrared reflectance of anisotropic (110) YBa₂Cu₃O₇ epitaxial film. *Solid State Communications* **70**, 547-551 (1989).
- ²⁰ J. Petzelt, S. Kamba, and J. Hlinka, Ferroelectric soft modes in ceramics and films, review in *New Development in Advanced Functional Ceramics*, Ed. L. Mitoseriu, Transworld Research Network, Trivandrum 2007, p. 387-421
- ²¹ S. Kamba, E. Buixaderas, T. Ostapchuk, and J. Petzelt. Ferroelectric soft modes and dynamic central modes near some phase transitions. *Ferroelectrics* **268**, 163-168 (2002).
- ²² R. H. Lyddane, R. G. Sachs, and E. Teller. On the Polar Vibrations of Alkali Halides. *Phys. Rev.* **59**, 673-676 (1941).
- ²³ J. Hlinka, B. Hehlen, A. Kania, and I. Gregora. Soft mode in cubic PbTiO₃ by hyper-Raman scattering. *Phys. Rev. B* **87**, 064101 (2013).
- ²⁴ H. Vogt. Refined treatment of the model of linearly coupled anharmonic oscillators and its application to the temperature dependence of the zone-center soft-mode frequencies of KTaO₃ and SrTiO₃. *Phys. Rev. B* **51**, 8046-8059 (1995).
- ²⁵ J. Petzelt, T. Ostapchuk, I. Gregora, I. Rychetsky, S. Hoffmann-Eifert, A. Pronin, Y. Yuzyuk, B. Gorshunov, S. Kamba, V. Bovtun, J. Pokorny, M. Savinov, V. Porokhonsky, D. Rafaja, P. Vanek, A. Almeida, M. Chaves, A. Volkov, M. Dressel, and R. Waser. Dielectric, infrared, and Raman response of undoped SrTiO₃ ceramics: Evidence of polar grain boundaries. *Phys. Rev. B* **64**, 184111 (2001).
- ²⁶ Y. Ichikawa, M. Nagai, and K. Tanaka. Direct observation of the soft-mode dispersion in the incipient ferroelectric KTaO₃. *Phys. Rev. B* **71**, 092106 (2005).
- ²⁷ E. Buixaderas, S. Kamba, I. Gregora, P. Vanek, J. Petzelt, T. Yamaguchi, and M. Wada. Far-infrared and Raman studies of the ferroelectric phase transition in LiNaGe₄O₉. *Physica Status Solidi B-Basic Research* **214**, 441-452 (1999).
- ²⁸ G.V. Kozlov, A.A. Volkov, J.F. Scott, G.E. Feldkamp, and J. Petzelt. Millimeter-wavelength spectroscopy of the ferroelectric phase transition in tris-sarcosine calcium chloride. *Phys. Rev. B* **28**, 255-261 (1983).
- ²⁹ S. Kamba, J. Petzelt, V. Dvořák, Y. Goncharov, A. A. Volkov, G. V. Kozlov, and J. Albers. Far infrared spectroscopy of the phase-transition sequence in BCCD. *Ferroelectrics* **105**, 351-356 (1990).
- ³⁰ S. Kamba, G. Schaack, and J. Petzelt. **Vibrational spectroscopy and soft-mode behavior in Rochelle Salt.** *Phys. Rev. B* **51**, 14998-15007 (1995).
- ³¹ E. Buixaderas, S. Kamba, and J. Petzelt. Lattice dynamics and central-mode phenomena in the dielectric response of ferroelectrics and related materials. *Ferroelectrics* **308**, 131-192 (2004).
- ³² J. Valasek. Piezoelectric and allied phenomena in Rochelle salt. *Phys. Rev.* **15**, 537-538 (1920).
- ³³ J. Valasek. Piezo-electric and allied phenomena in Rochelle salt. *Phys. Rev.* **17**, 475-481 (1921).
- ³⁴ Y. Iwata, S. Mitani, and I. Shibuya. Neutron diffraction analysis on a possible disordered structure of paraelectric rochelle salt. *Ferroelectrics* **107**, 287-292 (1990).
- ³⁵ F. Mo, R. H. Mathiesen, J. A. Beukes, and K. M. Vu. Rochelle salt - a structural reinvestigation with improved tools. I. The high-temperature para-electric phase at 308 K. *IUCrJ* **2**, 19-28 (2015).
- ³⁶ H. Akao and T. Sasaki. Dielectric dispersion of Rochelle salt in the microwave region. *J. Chem. Phys.* **23**, 2210-2214 (1955).
- ³⁷ H. E. Müser and J. Pottharst. Zum dielektrischen Vorhalten von Seignettesalz im Bereich der Dezimeter- und Zentimeterwellen. *Phys. Stat. Sol.* **24**, 109-113 (1967).
- ³⁸ F. Sandy and R. V. Jones. Dielectric Relaxation of Rochelle Salt. *Physical Review* **168**, 481-493 (1968).
- ³⁹ M. Horioka, Y. Satuma, and H. Yanagihara. Dielectric dispersion and soft mode in Rochelle salt. *J. Phys. Soc. Jpn.* **62**, 2233-2236 (1993).
- ⁴⁰ A.A. Volkov, G.V. Kozlov, E.B. Kryukova, and J. Petzelt. Low-temperature transformations of the relaxational soft modes in crystals of the Rochelle salt family. *Sov. Phys. JETP* **63**, 110-114 (1986).

- ⁴¹ A.A. Volkov, G.V. Kozlov, E.B. Kryukova, and A.A. Sobyenin, New results on the dynamics of Rochelle salt crystals (a system with a "double" critical point)," *Sov. Phys. Usp.* **29**, 574-575 (1986)
- ⁴² J. Hlinka, J. Kulda, S. Kamba, and J. Petzelt. Resonant soft mode in Rochelle salt by inelastic neutron scattering. *Phys. Rev. B* **63** 052102 (2001).
- ⁴³ S. Kamba, G. Schaack, J. Petzelt, and B. Brezina. Soft-mode behaviour in Rochelle Salt and Lithium Thallium Tartrate Monohydrate at high pressure. *Ferroelectrics* **186**, 181 (1996).
- ⁴⁴ B. T. Matthias and J. K. Hulm. New Ferroelectric Tartrates. *Physical Review* **82**, 108-109 (1951).
- ⁴⁵ J. Fousek, L. E. Cross, and K. Seely. Some properties of the ferroelectric lithium thallium tartrate. *Ferroelectrics* **1**, 63-70 (1970).
- ⁴⁶ E. Sawaguchi and L.E. Cross. Electromechanical coupling effects on the dielectric properties and ferroelectric phase transition in lithium thallium tartrate. *Ferroelectrics* **2**, 37-46 (1971).
- ⁴⁷ X. Gerbaux, A. Hadni, J. Pierron, and S. Messaadi. Soft mode and far infrared spectra of ferroelectric Lithium Thallium Tartrate at low temperatures. *Int. J. Infrared Millimeter Waves* **6**, 131-140 (1985).
- ⁴⁸ A.A. Volkov, Yu.G. Goncharov, G.V. Kozlov, J. Petzelt, J. Fousek, and B. Brezina, Temperature unstable mode in the submillimeter wavelength spectrum of lithium-thallium tartrate, *Sov. Phys. Sol. State* **28**, 1794 (1986).
- ⁴⁹ K. Hayashi, K. Deguchi, and E. Nakamura. Elastic and dielectric studies on the phase transition of Ferroelectric $\text{LiTiC}_4\text{H}_4\text{O}_6 \cdot \text{H}_2\text{O}$. *J. Phy. Soc. Jpn.* **61**, 1357-1361 (1992).
- ⁵⁰ G. J. McCarthy, L. H. Schlegel, and E. Sawaguchi. Crystal data for lithium thallium tartrate monohydrate. *J. Appl. Cryst.* **4**, 180-181 (1971).
- ⁵¹ M. I. Kay. The structure of the paraelectric phase of lithium thallium tartrate monohydrate by neutron diffraction data. *Ferroelectrics* **19**, 159-164 (1978).
- ⁵² S. Kamba, G. Schaack, J. Petzelt, and B. Brezina. High-pressure dielectric and lattice vibration studies of the phase transition in lithium thallium tartrate monohydrate (LTT). *J Phys-Condens Mat* **8**, 4631-4642 (1996).
- ⁵³ A. K. Tagantsev. Susceptibility Anomaly in Films with Bilinear Coupling between Order Parameter and Strain. *Phys Rev Lett* **94**, 247603 (2005).
- ⁵⁴ S. Kamba, J. Kulda, V. Petříček, G. McIntyre, and J. Kiat. High-pressure structural and dielectric studies of the phase transitions in lithium thallium tartrate monohydrate. *J Phys-Condens Mat* **14**, 4045-4055 (2002).
- ⁵⁵ S. Kamba, B. Brezina, J. Petzelt, and G. Schaack. Study of the phase transition in lithium ammonium tartrate monohydrate (LAT) by means of infrared and Raman spectroscopy. *J. Phys.: Condens. Matter* **8**, 8669-8679 (1996).
- ⁵⁶ G. A. Smolenskii and A. I. Agranovskaya, *Soviet Phys. – Tech. Phys.* **3**, 1380 (1958).
- ⁵⁷ V. A. Isupov, Causes of phase-transition broadening and the nature of dielectric polarization in some ferroelectrics, *Sov. Phys.-Sol. State* **5**, 136-140 (1963)
- ⁵⁸ N. De Mathan, E. Husson, G. Calvarin, J. R. Gavarrin, A. W. Hewat, and A. Morell. A structural model for the relaxor $\text{PbMg}_{1/3}\text{Nb}_{2/3}\text{O}_3$ at 5 K. *J. Phys.: Condens. Matter* **3**, 8159-8171 (1991).
- ⁵⁹ G. Calvarin, E. Husson, and Z. G. Ye. X-ray study of the electric field-induced phase transition in single crystal $\text{Pb}(\text{Mg}_{1/3}\text{Nb}_{2/3})\text{O}_3$. *Ferroelectrics* **165**, 349-358 (1995).
- ⁶⁰ G. Burns and F. H. Dacol. Glassy polarization behavior in ferroelectric compounds $\text{Pb}(\text{Mg}_{1/3}\text{Nb}_{2/3})\text{O}_3$ and $\text{Pb}(\text{Zn}_{1/3}\text{Nb}_{2/3})\text{O}_3$. *Sol. State Commun.* **48**, 853-856 (1983).
- ⁶¹ V. Westphal, W. Kleemann, and M. D. Glinchuk. Diffuse Phase-Transitions and Random-Field-Induced Domain States of the Relaxor Ferroelectric $\text{PbMg}_{1/3}\text{Nb}_{2/3}\text{O}_3$. *Phys Rev Lett* **68**, 847-850 (1992).
- ⁶² S.-E. Park and T. R. ShROUT. Ultrahigh strain and piezoelectric behavior in relaxor based ferroelectric single crystals. *J Appl Phys* **82**, 1804-1811 (1997).
- ⁶³ L. E. Cross. Relaxor ferroelectrics. *Ferroelectrics* **76**, 241-267 (1987).
- ⁶⁴ L. E. Cross. Relaxor ferroelectrics: An overview. *Ferroelectrics* **151**, 305-320 (1994).
- ⁶⁵ Z.-G. Ye, edited by C. Boulesteix, in *Key Engineering Materials*, Vols. **155-156**, 81-122 (1998). Trans Tech Publications, Switzerland
- ⁶⁶ G.A. Samara, "Ferroelectricity Revisited-Advances in Materials and Physics." Edited by H. Ehrenreich, F. Spaepen, in *Solid State Physics, Advances in Research and Applications*. Vol. **56**. (San Diego: Academic Press, 2001), pp. 240-458.
- ⁶⁷ G.A. Samara. The relaxational properties of compositionally disordered ABO_3 perovskites. *J. Phys.: Condens. Matter* **15**, R367-R411 (2003).
- ⁶⁸ A. A. Bokov and Z. G. Ye. Recent progress in relaxor ferroelectrics with perovskite structure. *J. Mat. Sci.* **41**, 31-52 (2006).
- ⁶⁹ A. A. Bokov and Z.-G. Ye. Dielectric Relaxation in Relaxor Ferroelectrics. *J. Adv. Diel.* **02**, 1241010 (2012).
- ⁷⁰ I. G. Siny, R. S. Katiyar, and A. S. Bhalla, *Ferroelectrics Review* **2**, 51 (2000).
- ⁷¹ G. Shirane and P. M. Gehring, in *Morphotropic Phase Boundary Perovskites, High Strain Piezoelectrics, and Dielectric Ceramics*, edited by R. Guo, K. M. Nair, W. Wong-Ng, A. Bhalla, D. Viehland, D. Suvorov, C. Wu and S.-I. Hirano, in *Ceramic Transactions* **136**, pp. 17-35 (2003) The American Ceramic Society.

- ⁷² R. A. Cowley, S. N. Gvasaliya, S. G. Lushnikov, B. Roessli, and G. M. Rotaru. Relaxing with relaxors: a review of relaxor ferroelectrics. *Adv. Phys.* **60**, 229-327 (2011).
- ⁷³ S. Kamba and J. Petzelt, in *Piezoelectric Single Crystals and Their Application*, edited by S. Trolier-McKinstry, L.E. Cross, and Y. Yamashita, (Penn State University, 2004), pp. 257-275.
- ⁷⁴ J. Hlinka, J. Petzelt, S. Kamba, D. Noujni, and T. Ostapchuk. Infrared dielectric response of relaxor ferroelectrics. *Phase Transitions* **79**, 41-78 (2006).
- ⁷⁵ S. Kamba, V. Bovtun, J. Petzelt, I. Rychetsky, R. Mizaras, A. Brilingas, J. Banys, J. Grigas, and M. Kosec. Dielectric dispersion of the relaxor PLZT ceramics in the frequency range 20 Hz-100 THz. *J. Phys.: Condens. Matter* **12**, 497-519 (2000).
- ⁷⁶ I. Rychetsky, S. Kamba, V. Porokhonsky, A. Pashkin, M. Savinov, V. Bovtun, J. Petzelt, M. Kosec, and M. Dressel. Frequency-independent dielectric losses (1/f noise) in PLZT relaxors at low temperatures. *J. Physics: Condens. Matter* **15**, 6017-6030 (2003).
- ⁷⁷ S. Kamba, D. Nuzhnyy, S. Veljko, V. Bovtun, J. Petzelt, Y. L. Wang, N. Setter, J. Levoska, M. Tyunina, J. Macutkevici, and J. Banys. Dielectric relaxation and polar phonon softening in relaxor ferroelectric $\text{PbMg}_{1/3}\text{Ta}_{2/3}\text{O}_3$. *J. Appl. Phys.* **102**, 074106 (2007).
- ⁷⁸ S. Kamba, V. Porokhonsky, A. Pashkin, V. Bovtun, J. Petzelt, J. Nino, S. Trolier-Mckinstry, M. Lanagan, and C. Randall. Anomalous broad dielectric relaxation in $\text{Bi}_{1.5}\text{Zn}_{1.0}\text{Nb}_{1.5}\text{O}_7$ pyrochlore. *Phys. Rev. B* **66** 054106 (2002).
- ⁷⁹ V. Bovtun, S. Vejko, S. Kamba, J. Petzelt, S. Vakhrushev, Y. Yakymenko, K. Brinkman, and N. Setter. Broad-band dielectric response of $\text{PbMg}_{1/3}\text{Nb}_{2/3}\text{O}_3$ relaxor ferroelectrics: Single crystals, ceramics and thin films. *J. Europ. Ceram. Soc.* **26**, 2867-2875 (2006).
- ⁸⁰ V. Bovtun, S. Kamba, A. Pashkin, M. Savinov, P. Samoukhina, J. Petzelt, I.P. Bykov, and M.A. Glinchuk. Central-peak components and polar soft mode in relaxor $\text{PbMg}_{1/3}\text{Nb}_{2/3}\text{O}_3$ crystals. *Ferroelectrics* **298**, 23-30 (2004).
- ⁸¹ V. Bovtun, J. Petzelt, V. Porokhonsky, S. Kamba, and Y. Yakymenko. Structure of the dielectric spectrum of relaxor ferroelectrics. *J. Eur. Ceram. Soc.* **21**, 1307-1311 (2001).
- ⁸² D. Nuzhnyy, J. Petzelt, V. Bovtun, M. Kempa, S. Kamba, and J. Hlinka. Infrared, terahertz, and microwave spectroscopy of the soft and central modes in $\text{Pb}(\text{Mg}_{1/3}\text{Nb}_{2/3})\text{O}_3$. *Phys. Rev. B* **96**, 174113 (2017).
- ⁸³ S. Wakimoto, C. Stock, R. J. Birgeneau, Z. G. Ye, W. Chen, W. J. L. Buyers, P. M. Gehring, and G. Shirane. Ferroelectric ordering in the relaxor $\text{Pb}(\text{Mg}_{1/3}\text{Nb}_{2/3})\text{O}_3$ as evidenced by low-temperature phonon anomalies. *Phys. Rev. B* **65**, 172105 (2002).
- ⁸⁴ P. Gehring, S.-E. Park, and G. Shirane. Soft phonon anomalies in the relaxor ferroelectric $\text{Pb}(\text{Zn}_{1/3}\text{Nb}_{2/3})_{0.92}\text{Ti}_{0.08}\text{O}_3$. *Phys Rev Lett* **84**, 5216 (2000).
- ⁸⁵ P. M. Gehring, S. Wakimoto, Z. G. Ye, and G. Shirane. Soft mode dynamics above and below the Burns temperature in the relaxor $\text{Pb}(\text{Mg}_{1/3}\text{Nb}_{2/3})\text{O}_3$. *Phys. Rev. Lett.* **87**, 277601 (2001).
- ⁸⁶ J. Hlinka, S. Kamba, J. Petzelt, J. Kulda, C. Randall, and S. Zhang. Origin of the "Waterfall" effect in phonon dispersion of relaxor perovskites. *Phys. Rev. Lett.* **91**, 107602 (2003).
- ⁸⁷ S. Kamba, M. Kempa, V. Bovtun, J. Petzelt, K. Brinkman, and N. Setter. Soft and central mode behaviour in $\text{PbMg}_{1/3}\text{Nb}_{2/3}\text{O}_3$ relaxor ferroelectric. *J. Phys.: Condens. Matter* **17**, 3965-3974 (2005).
- ⁸⁸ S. Kamba, M. Berta, M. Kempa, J. Hlinka, J. Petzelt, K. Brinkman, and N. Setter. Far-infrared soft-mode behavior in $\text{PbSc}_{1/2}\text{Ta}_{1/2}\text{O}_3$ thin films. *J Appl Phys* **98**, 074103 (2005).
- ⁸⁹ D. Nuzhnyy, J. Petzelt, V. Bovtun, S. Kamba, and J. Hlinka. Soft mode driven local ferroelectric transition in lead-based relaxors. *Appl. Phys. Lett.* **114**, 182901 (2019).
- ⁹⁰ D. Viehland, S. J. Jang, L. E. Cross, and M. Wuttig. Deviation from Curie-Weiss behavior in relaxor ferroelectrics. *Phys. Rev. B* **46**, 8003-8006 (1992).
- ⁹¹ J. H. Haeni, P. Irvin, W. Chang, R. Uecker, P. Reiche, Y. L. Li, and A. K. Tagantsev. Room-temperature ferroelectricity in strained SrTiO_3 . *Nature* **430**, 758-761 (2004).
- ⁹² D. Nuzhnyy, J. Petzelt, S. Kamba, P. Kuzel, C. Kadlec, V. Bovtun, M. Kempa, J. Schubert, C. M. Brooks, and D. G. Schlom. Soft mode behavior in $\text{SrTiO}_3/\text{DyScO}_3$ thin films: Evidence of ferroelectric and antiferrodistortive phase transitions. *Appl. Phys. Lett.* **95**, 232902 (2009).
- ⁹³ C.-H. Lee, V. Skoromets, M. D. Biegalski, S. Lei, R. Haislmaier, M. Bernhagen, R. Uecker, X. Xi, V. Gopalan, X. Marti, S. Kamba, P. Kuzel, and D. G. Schlom. Effect of stoichiometry on the dielectric properties and soft mode behavior of strained epitaxial SrTiO_3 thin films on DyScO_3 substrates. *Appl. Phys. Lett.* **102**, 082905 (2013).
- ⁹⁴ D. Nuzhnyy, J. Petzelt, S. Kamba, X. Marti, T. Cechal, C. M. Brooks, and D. G. Schlom. Infrared phonon spectroscopy of a compressively strained (001) SrTiO_3 film grown on a (110) NdGaO_3 substrate. *J Phys-Condens Mat* **23**, 045901 (2011).
- ⁹⁵ D. Nuzhnyy, J. Petzelt, S. Kamba, T. Yamada, M. Tyunina, A. K. Tagantsev, J. Levoska, and N. Setter. Polar phonons in some compressively stressed epitaxial and polycrystalline SrTiO_3 thin films. *J. Electroceram.* **22**, 297-301 (2009).

- ⁹⁶ R. C. Haislmaier, R. Engel-Herbert, and V. Gopalan. Stoichiometry as key to ferroelectricity in compressively strained SrTiO₃ films. *Appl. Phys. Lett.* **109**, 032901 (2016).
- ⁹⁷ J. Petzelt and S. Kamba. Far infrared and terahertz spectroscopy of ferroelectric soft modes in thin films: A review. *Ferroelectrics* **503**, 19-44 (2016).
- ⁹⁸ S. Kamba, P. Samoukhina, F. Kadlec, J. Pokorny, J. Petzelt, I. Reaney, and P. Wise. Composition dependence of the lattice vibrations in Sr_{n+1}Ti_nO_{3n+1} Ruddlesden-Popper homologous series. *J Eur Ceram Soc* **23**, 2639-2645 (2003).
- ⁹⁹ D. Noujni, S. Kamba, A. Pashkin, V. Bovtun, J. Petzelt, A.-K. Axelsson, N.M. Alford, P.L. Wise, I.M. Reaney, Temperature dependence of microwave and THz dielectric response in Sr_{n+1}Ti_nO_{3n+1} (n=1-4), *Integrated Ferroelectrics* **62**, 199-203 (2004).
- ¹⁰⁰ C.-H. Lee, N. D. Orloff, T. Birol, Y. Zhu, V. Goian, E. Rocas, R. Haislmaier, E. Vlahos, J. A. Mundy, L. F. Kourkoutis, Y. Nie, M. D. Biegalski, J. Zhang, M. Bernhagen, N. A. Benedek, Y. Kim, J. D. Brock, R. Uecker, X. X. Xi, V. Gopalan, D. Nuzhnyy, S. Kamba, D. A. Muller, I. Takeuchi, J. C. Booth, C. J. Fennie, D. G. Schlom: Exploiting dimensionality and defect mitigation to create tunable microwave dielectrics, *Nature* **502**, 532-536 (2013).
- ¹⁰¹ V. Goian, S. Kamba, N. Orloff, T. Birol, C. H. Lee, D. Nuzhnyy, J. C. Booth, M. Bernhagen, R. Uecker, D. G. Schlom, Influence of the central mode and soft phonon on the microwave dielectric loss near the strain-induced ferroelectric phase transitions in Sr_{n+1}Ti_nO_{3n+1} *Phys. Rev. B* **90**, 174105 (2014).
- ¹⁰² N. M. Dawley, E. J. Marks, A. M. Hagerstrom, G. H. Olsen, M. E. Holtz, V. Goian, C. Kadlec, J. Zhang, X. Lu, J. A. Drisko, R. Uecker, S. Ganschow, C. J. Long, J. C. Booth, S. Kamba, C. J. Fennie, D. A. Muller, N. D. Orloff, and D. G. Schlom. Targeted chemical pressure yields tuneable millimetre-wave dielectric. *Nature Mater.* **19**, 176-181 (2020).
- ¹⁰³ V. Železný, J. Buršík, P. Vaněk: Preparation and infrared characterization of potassium tantalate thin films, *J. Eur. Ceram. Soc.* **25**, 2155-2159 (2005).
- ¹⁰⁴ V. Skoromets, S. Glinšek, V. Bovtun, M. Kempa, J. Petzelt, S. Kamba, B. Malič, M. Kosec, P. Kužel: Ferroelectric phase transition in polycrystalline KTaO₃ thin film revealed by terahertz spectroscopy, *Appl. Phys. Lett.* **99**, 052908 (2011).
- ¹⁰⁵ S. Glinšek, D. Nuzhnyy, J. Petzelt, B. Malič, S. Kamba, V. Bovtun, M. Kempa, V. Skoromets, P. Kužel, I. Gregora, M. Kosec, Lattice dynamics and broad-band dielectric properties of the KTaO₃ ceramics, *J. Appl. Phys.* **111**, 104101 (2012).
- ¹⁰⁶ S. Kamba, D. Nuzhnyy, M. Savinov, J. Šebek, J. Petzelt, J. Prokleška, R. Haumont, and J. Kreisel. Infrared and terahertz studies of polar phonons and magnetodielectric effect in multiferroic BiFeO₃ ceramics. *Phys. Rev. B* **75**, 024403 (2007).
- ¹⁰⁷ Y. F. Popov, A. M. Kadomtseva, G. P. Vorob'ev, and A. K. Zvezdin. Discovery of the linear magnetoelectric effect in magnetic ferroelectric BiFeO₃ in a strong magnetic field. *Ferroelectrics* **162**, 135-140 (1994).
- ¹⁰⁸ I. A. Kornev, S. Lisenkov, R. Haumont, B. Dkhil, and L. Bellaiche. Finite-temperature properties of multiferroic BiFeO₃. *Phys. Rev. Lett.* **99**, 227602 (2007).
- ¹⁰⁹ S. Skiadopoulou, V. Goian, C. Kadlec, F. Kadlec, X. F. Bai, I. C. Infante, B. Dkhil, C. Adamo, D. G. Schlom, and S. Kamba. Spin and lattice excitations of a BiFeO₃ thin film and ceramics. *Phys. Rev. B* **91**, 174108 (2015).
- ¹¹⁰ I. Kezsmarki, U. Nagel, S. Bordacs, R. S. Fishman, J. H. Lee, H. T. Yi, S. W. Cheong, and T. Room. Optical Diode Effect at Spin-Wave Excitations of the Room-Temperature Multiferroic BiFeO₃. *Phys. Rev. Lett.* **115**, 127203-127205 (2015).
- ¹¹¹ M. Cazayous, Y. Gallais, A. Sacuto, R. De Sousa, D. Lebeugle, and D. Colson. Possible observation of cycloidal electromagnons in BiFeO₃. *Phys. Rev. Lett.* **101**, 037601-037604 (2008).
- ¹¹² C. J. Fennie, K. M. Rabe: Magnetic and Electric Phase Control in Epitaxial EuTiO₃ from First Principles, *Phys. Rev. Lett.* **97**, 267602 (2006).
- ¹¹³ T. Katsufuji, H. Takagi: Coupling between magnetism and dielectric properties in quantum paraelectric EuTiO₃, *Phys. Rev. B* **64**, 054415 (2001).
- ¹¹⁴ S. Kamba, D. Nuzhnyy, P. Vaněk, M. Savinov, K. Knížek, Z. Shen, E. Šantavá, K. Maca, M. Sadowski, J. Petzelt: Magnetodielectric effect and optic soft mode behaviour in quantum paraelectric EuTiO₃ ceramics, *Eur. Phys. Lett.* **80**, 27002 (2007).
- ¹¹⁵ V. Goian, S. Kamba, J. Hlinka, P. Vaněk, A. A. Belik, T. Kolodiazhnyi, J. Petzelt: Polar phonon mixing in magnetoelectric EuTiO₃, *Eur. Phys. J. B* **71**, 429-433 (2009).
- ¹¹⁶ V. Goian, S. Kamba, O. Pacherová, J. Drahoukoupil, L. Palatinus, M. Dušek, J. Rohlíček, M. Savinov, F. Laufek, W. Schranz, A. Fuith, M. Kachlík, K. Maca, A. Shkabko, L. Sagarna, A. Weidenkaff, A. A. Belik: Antiferrodistortive phase transition in EuTiO₃, *Phys. Rev. B* **86**, 054112 (2012).
- ¹¹⁷ J. Köhler, R. Dinnebier, and A. Bussmann-Holder: Structural instability of EuTiO₃ from X-ray powder diffraction, *Phase Transition*, **85**, 949-955 (2012).

- ¹¹⁸ J. H. Lee, L. Fang, E. Vlahos, X. Ke, Y. W. Jung, L. F. Kourkoutis, J.-W. Kim, P. J. Ryan, T. Heeg, M. Roeckerath, V. Goian, M. Bernhagen, R. Uecker, P. C. Hammel, K. M. Rabe, S. Kamba, J. Schubert, J. W. Freeland, D. A. Muller, C. J. Fennie, P. Schiffer, V. Gopalan, E. Johnston-Halperin, D. G. Schlom: A strong ferroelectric ferromagnet created by means of spin-lattice coupling, *Nature* **466**, 954-959 (2010).
- ¹¹⁹ J. H. Lee, L. Fang, E. Vlahos, X. Ke, Y. W. Jung, L. F. Kourkoutis, J.-W. Kim, P. J. Ryan, T. Heeg, M. Roeckerath, V. Goian, M. Bernhagen, R. Uecker, P. C. Hammel, K. M. Rabe, S. Kamba, J. Schubert, J. W. Freeland, D. A. Muller, C. J. Fennie, P. Schiffer, V. Gopalan, E. Johnston-Halperin, D. G. Schlom: Addendum to „A strong ferroelectric ferromagnet created by means of spin-lattice coupling“, *Nature* **476**, 114 (2011).
- ¹²⁰ S. Kamba, V. Goian, M. Orlita, D. Nuzhnyy, J. H. Lee, D. G. Schlom, K. Z. Rushchanskii, M. Lezaic, T. Birol, C. J. Fennie, P. Gemeiner, B. Dkhil, V. Bovtun, M. Kempa, J. Hlinka, J. Petzelt: Magnetodielectric effect and phonon properties of compressively strained EuTiO_3 thin films deposited on (001) $(\text{LaAlO}_3)_{0.29}$ - $(\text{SrAl}_{1/2}\text{Ta}_{1/2}\text{O}_3)_{0.71}$, *Phys. Rev. B* **85**, 094435 (2012).
- ¹²¹ K. Z. Rushchanskii, S. Kamba, V. Goian, P. Vaněk, M. Savinov, J. Prokleška, D. Nuzhnyy, K. Knížek, F. Laufek, S. Eckel, S. K. Lamoreaux, A. O. Sushkov, M. Lezaic, and N. A. Spaldin. A multiferroic material to search for the permanent electric dipole moment of the electron. *Nature Materials* **9**, 649-654 (2010).
- ¹²² V. Goian, S. Kamba, D. Nuzhnyy, P. Vaněk, M. Kempa, V. Bovtun, K. Knizek, J. Prokleska, F. Borodavka, M. Ledinsky, and I. Gregora. Dielectric, magnetic and structural properties of novel multiferroic ceramics. *J Phys-Condens Mat* **23**, 025904 (2011).
- ¹²³ V. Goian, S. Kamba, P. Vaněk, M. Savinov, C. Kadlec, and J. Prokleška. Magnetic and dielectric properties of multiferroic $\text{Eu}_{0.5}\text{Ba}_{0.25}\text{Sr}_{0.25}\text{TiO}_3$ ceramics. *Phase Transitions* **86**, 191-199 (2013).
- ¹²⁴ S. Eckel, A. O. Sushkov, and S. K. Lamoreaux. Limit on the electron electric dipole moment using paramagnetic ferroelectric $\text{Eu}_{0.5}\text{Ba}_{0.5}\text{TiO}_3$. *Phys. Rev. Lett.* **109**, 193003 (2012).
- ¹²⁵ E. Bousquet, N. A. Spaldin, and P. Ghosez. Strain-induced ferroelectricity in simple rocksalt binary oxides. *Phys. Rev. Lett.* **104**, 037601-037604 (2010).
- ¹²⁶ V. Goian, R. Held, E. Bousquet, Y. Yuan, A. Melville, H. Zhou, V. Gopalan, P. Ghosez, N.A. Spaldin, D.G. Schlom, and S. Kamba, Making EuO multiferroic by epitaxial strain engineering. *Communications Materials* **1**, 74 (2020).
- ¹²⁷ J. H. Lee, K. M. Rabe: Epitaxial-Strain-Induced Multiferroicity in SrMnO_3 from First Principles, *Phys. Rev. Lett.* **104**, 207204 (2010).
- ¹²⁸ S. Kamba, V. Goian, V. Skoromets, J. Hejtmánek, V. Bovtun, M. Kempa, F. Borodavka, P. Vaněk, A. A. Belik, J. H. Lee, O. Pacherová, and K. M. Rabe. Strong spin-phonon coupling in infrared and Raman spectra of SrMnO_3 . *Phys. Rev. B* **89**, 064308 (2014).
- ¹²⁹ C. Becher *et al.* Strain-induced coupling of electrical polarization and structural defects in SrMnO_3 films. *Nat. Nanotech.* **10**, 661-665 (2015).
- ¹³⁰ H. Sakai, J. Fujioka, T. Fukuda, D. Okuyama, D. Hashizume, F. Kagawa, H. Nakao, Y. Murakami, T. Arima, A. Q. R. Baron, Y. Taguchi, and Y. Tokura. Displacement-Type Ferroelectricity with Off-Center Magnetic Ions in Perovskite $\text{Sr}_{1-x}\text{Ba}_x\text{MnO}_3$. *Phys. Rev. Lett.* **107**, 137601 (2011).
- ¹³¹ V. Goian, F. Kadlec, C. Kadlec, B. Dabrowski, S. Kolesnik, O. Chmaissem, D. Nuzhnyy, M. Kempa, V. Bovtun, M. Savinov, J. Hejtmánek, J. Prokleška, and S. Kamba. Spectroscopic studies of the ferroelectric and magnetic phase transitions in multiferroic $\text{Sr}_{1-x}\text{Ba}_x\text{MnO}_3$. *J. Phys.: Condens. Matter* **28**, 175901 (2016).
- ¹³² H. Sakai, J. Fujioka, T. Fukuda, M. S. Bahramy, D. Okuyama, R. Arita, T. Arima, A. Q. R. Baron, Y. Taguchi, and Y. Tokura. Soft phonon mode coupled with antiferromagnetic order in incipient-ferroelectric Mott insulators $\text{Sr}_{1-x}\text{Ba}_x\text{MnO}_3$. *Phys. Rev. B* **86**, 104407 (2012).
- ¹³³ C. J. Fennie and K. M. Rabe. Ferroelectric transition in YMnO_3 from first principles. *Phys. Rev. B* **72**, 100103(R) (2005).
- ¹³⁴ S. Kamba, D. Nuzhnyy, M. Savinov, P. Toledano, V. Laguta, P. Brazda, L. Palatinus, F. Kadlec, F. Borodavka, C. Kadlec, P. Bednyakov, V. Bovtun, M. Kempa, D. Kriegner, J. Drahokoupil, J. Kroupa, J. Prokleska, K. Chapagain, B. Dabrowski, and V. Goian. Unusual ferroelectric and magnetic phases in multiferroic 2H- BaMnO_3 ceramics. *Phys. Rev. B* **95**, 174103 (2017).
- ¹³⁵ J. Varignon and P. Ghosez. Improper ferroelectricity and multiferroism in 2H- BaMnO_3 . *Phys. Rev. B* **87**, 140403(R) (2013).
- ¹³⁶ T. Kimura, T. Goto, H. Shintani, K. Ishizaka, T. Arima, and Y. Tokura. Magnetic control of FE polarization. *Nature* **426**, 55-58 (2003).
- ¹³⁷ Y. Tokura, S. Seki, and N. Nagaosa. Multiferroics of spin origin. *Rep. Prog. Phys.* **77**, 076501 (2014).
- ¹³⁸ P. Tolédano. Pseudo-proper ferroelectricity and magnetoelectric effects in TbMnO_3 . *Phys. Rev. B* **79** (2009).
- ¹³⁹ D. Niermann, C. P. Grams, P. Becker, L. Bohaty, H. Schenck, and J. Hemberger. Critical slowing down near the multiferroic phase transition in MnWO_4 . *Phys. Rev. Lett.* **114**, 037204 (2015).
- ¹⁴⁰ A. Pimenov, A. A. Mukhin, V. Y. Ivanov, V. D. Travkin, A. M. Balbashov, and A. Loidl. Possible evidence for electromagnons in multiferroic manganites. *Nat. Phys.* **2**, 97-100 (2006).

-
- ¹⁴¹ C. Kadlec, F. Kadlec, V. Goian, M. Gich, M. Kempa, S. Rols, M. Savinov, J. Prokleska, M. Orlita, and S. Kamba. Electromagnon in ferrimagnetic epsilon-Fe₂O₃ nanograin ceramics. *Phys. Rev. B* **88**, 104301 (2013).
- ¹⁴² S. Skiadopoulou, F. Borodavka, C. Kadlec, F. Kadlec, M. Retuerto, Z. Deng, M. Greenblatt, and S. Kamba. Magnetolectric excitations in multiferroic Ni₃TeO₆. *Phys. Rev. B* **95**, 184435 (2017).
- ¹⁴³ S. Skiadopoulou, M. Retuerto, F. Borodavka, C. Kadlec, F. Kadlec, M. Mišek, J. Prokleška, Z. Deng, X. Tan, C. Frank, J. A. Alonso, M. T. Fernandez-Diaz, M. Croft, F. Orlandi, P. Manuel, E. McCabe, D. Legut, M. Greenblatt, and S. Kamba. Structural, magnetic, and spin dynamical properties of the polar antiferromagnets Ni_{3-x}Co_xTeO₆ (x=1,2). *Phys. Rev. B* **101**, 014429 (2020).
- ¹⁴⁴ F. Kadlec, V. Goian, C. Kadlec, M. Kempa, P. Vaněk, J. Taylor, S. Rols, J. Prokleška, M. Orlita, and S. Kamba. Possible coupling between magnons and phonons in multiferroic CaMn₇O₁₂. *Phys. Rev. B* **90**, 054307 (2014).
- ¹⁴⁵ S. Kamba, V. Goian, F. Kadlec, D. Nuzhnyy, C. Kadlec, J. Vít, F. Borodavka, I. S. Glazkova, and A. A. Belik. Changes in spin and lattice dynamics induced by magnetic and structural phase transitions in multiferroic SrMn₇O₁₂. *Phys. Rev. B* **99**, 184108 (2019).
- ¹⁴⁶ J. Vít, F. Kadlec, C. Kadlec, F. Borodavka, Y. S. Chai, K. Zhai, Y. Sun, and S. Kamba. Electromagnon in the Y-type hexaferrite BaSrCoZnFe₁₁AlO₂₂. *Phys. Rev. B* **97**, 134406 (2018).
- ¹⁴⁷ F. Kadlec, C. Kadlec, J. Vít, F. Borodavka, M. Kempa, J. Prokleška, J. Buršík, R. Uhrecký, S. Rols, Y. S. Chai, K. Zhai, Y. Sun, J. Drahoukoupil, V. Goian, and S. Kamba. Electromagnon in the Z-type hexaferrite (Ba_xSr_{1-x})₃Co₂Fe₂₄O₄₁. *Phys. Rev. B* **94**, 024419 (2016).
- ¹⁴⁸ Y. S. Chai, S. H. Chun, J. Z. Cong, and K. H. Kim. Magnetolectricity in multiferroic hexaferrites as understood by crystal symmetry analyses. *Phys. Rev. B* **98**, 104416 (2018).
- ¹⁴⁹ K. Zhai, Y. Wu, S. Shen, W. Tian, H. Cao, Y. Chai, B. C. Chakoumakos, D. Shang, L. Yan, F. Wang, and Y. Sun. Giant magnetolectric effects achieved by tuning spin cone symmetry in Y-type hexaferrites. *Nature Commun.* **8**, 519 (2017).
- ¹⁵⁰ S. H. Chun, Y. S. Chai, B.-G. Jeon, H. J. Kim, Y. S. Oh, I. Kim, H. Kim, B. J. Jeon, S. Y. Haam, J.-Y. Park, S. H. Lee, J.-H. Chung, J.-H. Park, and K. H. Kim. Electric Field Control of Nonvolatile Four-State Magnetization at Room Temperature. *Phys. Rev. Lett.* **108**, 177201 (2012).
- ¹⁵¹ H. Shishikura, Y. Tokunaga, Y. Takahashi, R. Masuda, Y. Taguchi, Y. Kaneko, and Y. Tokura. Electromagnon Resonance at Room Temperature with Gigantic Magnetochromism. *Phys. Rev. Appl.* **9**, 044033 (2018).
- ¹⁵² S. H. Chun, K. W. Shin, H. J. Kim, S. Jung, J. Park, Y.-M. Bahk, H.-R. Park, J. Kyoung, D.-H. Choi, D.-S. Kim, G.-S. Park, J. F. Mitchell, and K. H. Kim. Electromagnon with Sensitive Terahertz Magnetochromism in a Room-Temperature Magnetolectric Hexaferrite. *Phys Rev Lett* **120**, 027202 (2018).
- ¹⁵³ V. Laguta, M. Kempa, V. Bovtun, J. Buršík, K. Zhai, Y. Sun, and S. Kamba. Magnetolectric coupling in multiferroic Z-type hexaferrite revealed by electric-field-modulated magnetic resonance studies. *J. Mat. Sci.* **55**, 7624-7633 (2020).
- ¹⁵⁴ R. D. Johnson, L. C. Chapon, D. D. Khalyavin, P. Manuel, P. G. Radaelli, and C. Martin. Giant Improper Ferroelectricity in the Ferroaxial Magnet CaMn₇O₁₂. *Phys Rev Lett* **108**, 067201 (2012).
- ¹⁵⁵ Y. S. Glazkova, N. Terada, Y. Matsushita, Y. Katsuya, M. Tanaka, A. V. Sobolev, I. A. Presniakov, and A. A. Belik. High-Pressure Synthesis, Crystal Structures, and Properties of CdMn₇O₁₂ and SrMn₇O₁₂ Perovskites. *Inorg. Chem.* **54**, 9081-9091 (2015).
- ¹⁵⁶ A. A. Belik, Y. S. Glazkova, N. Terada, Y. Matsushita, A. V. Sobolev, I. A. Presniakov, N. Tsujii, S. Nimori, K. Takehana, and Y. Imanaka. Spin-Driven Multiferroic Properties of PbMn₇O₁₂ Perovskite. *Inorg. Chem.* **55**, 6169-6177 (2016).

Selected most important publications and my contribution in these papers.

The thesis is based on the following articles. They are listed in a chronological order, which are referred to in the thesis.

1. S. Kamba, G. Schaack, and J. Petzelt. Vibrational spectroscopy and soft-mode behavior in Rochelle Salt. *Phys. Rev. B* **51**, 14998-15007 (1995). [cited 29x](#)
This work was created during my Humboldt scholarship at the University of Würzburg. I performed all IR and Raman spectroscopic measurements, evaluated the data and wrote the first version of the manuscript.
2. S. Kamba, G. Schaack, J. Petzelt, and B. Brezina. High-pressure dielectric and lattice vibration studies of the phase transition in lithium thallium tartrate monohydrate (LTT). *J Phys-Condens Mat* **8**, 4631-4642 (1996). [cited 7x](#)
This work was created during my Humboldt scholarship at the University of Würzburg. I performed all measurements, evaluated the data and wrote the first version of the manuscript.
3. S. Kamba, V. Bovtun, J. Petzelt, I. Rychetsky, R. Mizaras, A. Brilingas, J. Banys, J. Grigas, and M. Kosec. Dielectric dispersion of the relaxor PLZT ceramics in the frequency range 20 Hz-100 THz. *J. Phys.: Condens. Matter* **12**, 497-519 (2000). [cited 164x](#)
I performed the IR measurements, evaluated the spectra and participated in the writing of the manuscript. Microwave studies were performed by V. Bovtun and my Lithuanian colleagues, ceramics were provided by M. Kosec.
4. S. Kamba, V. Porokhonsky, A. Pashkin, V. Bovtun, J. Petzelt, J. Nino, S. Trolier-Mckinstry, M. Lanagan, and C. Randall. Anomalous broad dielectric relaxation in $\text{Bi}_{1.5}\text{Zn}_{1.0}\text{Nb}_{1.5}\text{O}_7$ pyrochlore. *Phys. Rev. B* **66** 054106 (2002). [cited 174x](#)
I performed the IR measurements, evaluated the spectra and wrote the first version of the manuscript. The microwave and THz measurements were performed by my colleagues from FZU, samples were provided by American collaborators.
5. S. Kamba, M. Kempa, V. Bovtun, J. Petzelt, K. Brinkman, and N. Setter. Soft and central mode behaviour in $\text{PbMg}_{1/3}\text{Nb}_{2/3}\text{O}_3$ relaxor ferroelectric. *J. Phys.: Condens. Matter* **17**, 3965-3974 (2005). [cited 89x](#)
I performed the IR measurements, evaluated the spectra and wrote the first version of the manuscript. The microwave and THz measurements were performed by my colleagues from FZU, samples were provided by Swiss collaborators.
6. D. Nuzhnyy, J. Petzelt, S. Kamba, P. Kužel, C. Kadlec, V. Bovtun, M. Kempa, J. Schubert, C. M. Brooks, and D. G. Schlom. Soft mode behavior in $\text{SrTiO}_3/\text{DyScO}_3$ thin films: Evidence of ferroelectric and antiferrodistortive phase transitions. *Appl. Phys. Lett.* **95**, 232902 (2009). [cited 36x](#)
I proposed the experiment, arranged the international cooperation, interpreted the IR spectra and participated in the writing of the manuscript. The thin films were provided by American collaborators, the measurements were performed by my colleagues from FZU.
7. S. Kamba, P. Samoukhina, F. Kadlec, J. Pokorny, J. Petzelt, I. Reaney, and P. Wise. Composition dependence of the lattice vibrations in $\text{Sr}_{n+1}\text{Ti}_n\text{O}_{3n+1}$ Ruddlesden-Popper homologous series. *J Eur Ceram Soc* **23**, 2639-2645 (2003). [cited 34x](#)
I led the research, interpreted the spectra and wrote the first version of the manuscript. Samples were provided by English collaborators.
8. C.-H. Lee, N. D. Orloff, T. Birol, Y. Zhu, V. Goian, E. Rocas, R. Haislmaier, E. Vlahos, J. A. Mundy, L. F. Kourkoutis, Y. Nie, M. D. Biegalski, J. Zhang, M. Bernhagen, N. A. Benedek, Y. Kim, J. D. Brock, R. Uecker, X. X. Xi, V. Gopalan, D. Nuzhnyy, S. Kamba, D. A. Muller, I. Takeuchi, J. C. Booth, C. J. Fennie, D. G. Schlom: Exploiting dimensionality and defect mitigation to create tunable microwave dielectrics, *Nature* **502**, 532-536 (2013). [cited 141x](#)

- American co-workers theoretically predicted strain-induced ferroelectric phase transition in $Sr_{n+1}Ti_nO_{3n+1}$, they grew thin films and measured microwave properties and second harmonic generation. I proposed the IR reflectance experiment (measured by V. Goian and D. Nuzhnyy from my group) which allowed me to explain the origin of observed low dielectric losses and the high tunability of dielectric permittivity. I also participated in writing of the manuscript.*
9. V. Goian, S. Kamba, N. Orloff, T. Birol, C. H. Lee, D. Nuzhnyy, J. C. Booth, M. Bernhagen, R. Uecker, D. G. Schlom, Influence of the central mode and soft phonon on the microwave dielectric loss near the strain-induced ferroelectric phase transitions in $Sr_{n+1}Ti_nO_{3n+1}$ *Phys. Rev. B* **90**, 174105 (2014). [cited 7x](#)
I proposed the IR experiment, interpreted the IR spectra and wrote the first version of the manuscript. The IR measurements were performed by my PhD student V. Goian, samples were provided by American collaborators.
 10. S. Kamba, D. Nuzhnyy, M. Savinov, J. Šebek, J. Petzelt, J. Prokleška, R. Haumont, and J. Kreisel. Infrared and terahertz studies of polar phonons and magnetodielectric effect in multiferroic $BiFeO_3$ ceramics. *Phys. Rev. B* **75**, 024403 (2007). [cited 222x](#)
I organized and led the research, interpreted experimental data and wrote the first version of the paper. Foreign co-authors provided us the samples.
 11. S. Skiadopoulou, V. Goian, C. Kadlec, F. Kadlec, X. F. Bai, I. C. Infante, B. Dkhil, C. Adamo, D. G. Schlom, and S. Kamba. Spin and lattice excitations of a $BiFeO_3$ thin film and ceramics. *Phys. Rev. B* **91**, 174108 (2015). [cited 22x](#)
I organized and led the research, interpreted experimental data and participated in writing of the manuscript. Foreign co-workers provided us the samples.
 12. S. Kamba, D. Nuzhnyy, P. Vaněk, M. Savinov, K. Knížek, Z. Shen, E. Šantavá, K. Maca, M. Sadowski, J. Petzelt: Magnetodielectric effect and optic soft mode behaviour in quantum paraelectric $EuTiO_3$ ceramics, *Eur. Phys. Lett.* **80**, 27002 (2007). [cited 72x](#)
I organized and led the research, interpreted experimental data and wrote the first version of the manuscript.
 13. V. Goian, S. Kamba, O. Pacherová, J. Drahokoupil, L. Palatinus, M. Dušek, J. Rohlíček, M. Savinov, F. Laufek, W. Schranz, A. Fuith, M. Kachlík, K. Maca, A. Shkabko, L. Sagarna, A. Weidenkaff, A. A. Belik: Antiferrodistortive phase transition in $EuTiO_3$, *Phys. Rev. B* **86**, 054112 (2012). [cited 72x](#)
I organized and led the research, interpreted experimental data and wrote the first version of the manuscript.
 14. J. H. Lee, L. Fang, E. Vlahos, X. Ke, Y. W. Jung, L. F. Kourkoutis, J.-W. Kim, P. J. Ryan, T. Heeg, M. Roeckerath, V. Goian, M. Bernhagen, R. Uecker, P. C. Hammel, K. M. Rabe, S. Kamba, J. Schubert, J. W. Freeland, D. A. Muller, C. J. Fennie, P. Schiffer, V. Gopalan, E. Johnston-Halperin, D. G. Schlom: A strong ferroelectric ferromagnet created by means of spin-lattice coupling, *Nature* **466**, 954-959 (2010). [cited 517x](#)
American co-workers theoretically predicted the strain-induced ferroelectric and ferromagnetic phase transition in $EuTiO_3$ thin films, they grew the thin films and measured second harmonic generation, structural and magnetic properties. I proposed the IR reflectance experiment (measured by my student V. Goian) for confirmation of the soft-mode driven ferroelectric phase transition, interpreted the data and wrote part of the manuscript.
 15. S. Kamba, V. Goian, M. Orlita, D. Nuzhnyy, J. H. Lee, D. G. Schlom, K. Z. Rushchanskii, M. Lezaic, T. Birol, C. J. Fennie, P. Gemeiner, B. Dkhil, V. Bovtun, M. Kempa, J. Hlinka, J. Petzelt: Magnetodielectric effect and phonon properties of compressively strained $EuTiO_3$ thin films deposited on (001) $(LaAlO_3)_{0.29}-(SrAl_{1/2}Ta_{1/2}O_3)_{0.71}$, *Phys. Rev. B* **85**, 094435 (2012). [cited 17x](#)
I organized and led the research, interpreted experimental data and wrote the first version of the manuscript. Foreign co-authors provided us the samples and calculated phonons in strained thin films.

16. K. Z. Rushchanskii, S. Kamba, V. Goian, P. Vaněk, M. Savinov, J. Prokleška, D. Nuzhnyy, K. Knížek, F. Laufek, S. Eckel, S. K. Lamoreaux, A. O. Sushkov, M. Ležaić, and N. A. Spaldin. A multiferroic material to search for the permanent electric dipole moment of the electron. *Nature Materials* **9**, 649-654 (2010). [cited 70x](#)
I organized and led the research in Prague, interpreted experimental data and participated in writing of the manuscript. Foreign co-workers made the theory.
17. V. Goian, R. Held, E. Bousquet, Y. Yuan, A. Melville, H. Zhou, V. Gopalan, P. Ghosez, N.A. Spaldin, D.G. Schlom, and S. Kamba, Making EuO multiferroic by epitaxial strain engineering. *Communications Materials* **1**, 74 (2020). [cited 1x](#)
I led the research in Prague, interpreted experimental data and wrote the first version of the manuscript. V. Goian measured the IR spectra, foreign co-authors made the theory, grew the strained thin films and superlattices and measured magnetic properties.
18. V. Goian, F. Kadlec, C. Kadlec, B. Dabrowski, S. Kolesnik, O. Chmaissem, D. Nuzhnyy, M. Kempa, V. Bovtun, M. Savinov, J. Hejtmánek, J. Prokleška, and S. Kamba. Spectroscopic studies of the ferroelectric and magnetic phase transitions in multiferroic $\text{Sr}_{1-x}\text{Ba}_x\text{MnO}_3$. *J. Phys.: Condens. Matter* **28**, 175901 (2016). [cited 9x](#)
I organized and led the research in Prague, interpreted experimental data and wrote the first version of the manuscript. Foreign co-authors provided us the samples.
19. S. Kamba, D. Nuzhnyy, M. Savinov, P. Toledano, V. Laguta, P. Brazda, L. Palatinus, F. Kadlec, F. Borodavka, C. Kadlec, P. Bednyakov, V. Bovtun, M. Kempa, D. Kriegner, J. Drahokoupil, J. Kroupa, J. Prokleška, K. Chapagain, B. Dabrowski, and V. Goian. Unusual ferroelectric and magnetic phases in multiferroic 2H-BaMnO₃ ceramics. *Phys. Rev. B* **95**, 174103 (2017). [cited 5x](#)
I organized and led the research in Prague, interpreted experimental data and wrote the first version of the manuscript. Foreign co-authors provided us the samples, P. Toledano wrote the part with the Landau theory.
20. S. Kamba, V. Goian, F. Kadlec, D. Nuzhnyy, C. Kadlec, J. Vít, F. Borodavka, I. S. Glazkova, and A. A. Belik. Changes in spin and lattice dynamics induced by magnetic and structural phase transitions in multiferroic $\text{SrMn}_7\text{O}_{12}$. *Phys. Rev. B* **99**, 184108 (2019). [cited 2x](#)
I organized and led the research in Prague, interpreted experimental data and wrote the first version of the manuscript. Foreign co-authors provided us the samples.
21. J. Vít, F. Kadlec, C. Kadlec, F. Borodavka, Y. S. Chai, K. Zhai, Y. Sun, and S. Kamba. Electromagnon in the Y-type hexaferrite $\text{BaSrCoZnFe}_{11}\text{AlO}_{22}$. *Phys. Rev. B* **97**, 134406 (2018). [cited 6x](#)
I organized and led the research in Prague, interpreted experimental data and participated in writing of the manuscript. My student J. Vít made most of the experiments, wrote the first version of the manuscript and developed the theory of IR activities of electromagnons in various magnetic structures. Foreign co-authors provided us the samples.